Intraband terms of magnetocrystalline anisotropy energy in layered systems without inversion symmetry

M. Cinal*

Institute of Physical Chemistry, Polish Academy of Sciences, 01-224 Warsaw, Poland

(Received 29 September 2023; revised 20 December 2023; accepted 21 December 2023; published 17 January 2024)

The origin of the intraband term of the magnetocrystalline anisotropy (MCA) energy, which has been shown to be present for layered systems without the inversion symmetry and be of similar magnitude as the interband term [M. Cinal, Phys. Rev. B **105**, 104403 (2022)], is investigated by considering a layered magnetic system perturbed by the spin-orbit coupling (SOC) at zero temperature. It is revealed that the second-order intraband contributions to the system band energy (the sum of the energies of occupied electron states), which are determined by the squares of the first-order corrections to electron energies at the Fermi surface (FS), actually result from small shifts of the FS sheets due to the SOC, the sheets being curves in the two-dimensional Brillouin zone. Thus, the intraband contributions to the band energy of the perturbed system, and, consequently, to the MCA energy defined as the difference of the band energies for two magnetization directions, come from the narrow stripelike regions of the Brillouin zone between the perturbed and unperturbed FS sheets for consecutive energy bands. In addition, the representation of the MCA energy as half the difference of the SOC energies for two magnetization directions, often used for spatial decomposition of this energy, is reexamined. It is shown that such an alternative representation, previously derived from the standard second-order perturbation-theory (PT) formula for the MCA energy which does not contain intraband terms [V. Antropov, L. Ke, and D. Åberg, Solid State Commun. **194**, 35 (2014)], is also valid in the absence of the inversion symmetry since the PT expansion of this representation includes, in fact, the intraband terms, and exactly reproduces the present extended second-order PT formula for the MCA energy. The theoretical findings are illustrated with the exemplary results for Co-based layered systems with and without the inversion symmetry: the Co film, the Co/Cu and Cu/Pd bilayers, as well as the Pd/Co/Pd trilayer.

DOI: 10.1103/PhysRevB.109.024424

I. INTRODUCTION

One of the key properties of magnetic systems is the magnetic anisotropy which determines the easy direction of magnetization and is vital for understanding observed magnetic structures and magnetization dynamics. The two sources of the magnetic anisotropy are the magnetic dipole-dipole interaction and the spin-orbit coupling (SOC). The former gives rise to the shape anisotropy determined by the system geometry while the latter leads to the magnetocrystalline anisotropy (MCA) which strongly depends on the electronic structure. Thus, in ultrathin layered systems the MCA energy depends not only on the type of interfaces and possible strain inside the layers but also the thicknesses of the constituent ferromagnetic and nonmagnetic layers. In particular, oscillations of the MCA energy have been found in theoretical calculations for Co, Fe, and Ni films [1–4], Co/X (X = Cu, Pd, and Pt) bilayers [2,5,6] as well as X/Co/X (X = Cu, Au, and Pd) trilayers [2,7–9]. The oscillatory thickness dependence has been shown [3,7,8,10] to result from pairs of quantum-well states, mainly built of d orbitals (s orbitals for Cu layers), with energies close to the Fermi energy while the oscillation periods are determined by the extremal dimensions of the Fermi surface of respective bulk materials as it was originally found for the interlayer exchange coupling in ferromagnet/nonmagnet/ferromagnet systems [11]. The presence of magnetic anisotropy oscillations and the predicted oscillation periods have been confirmed experimentally for magnetic layers on vicinal substrates [5,12–15]. The systems including a layer of Co in contact with a heavy metal, like Pd and Pt, and having the structure inversion asymmetry (i.e., the lack of the inversion symmetry) are currently of revived interest due to a high efficiency in switching of their magnetization with electric current via the spin-orbit torques and the presence of finite Dzyaloshinskii-Moriya interaction which can stabilize chiral magnetic structures like magnetic skyrmions (see, e.g., Refs. [16–22]).

The calculations of the MCA energy can be performed with various methods. In the standard approach, known as the force theorem (FT) [23,24], this energy is expressed as the difference of the system's band energies (obtained by summing the energies of occupied electron states) for two different magnetization directions, or the corresponding free energies at finite temperature, which are found with the Hamiltonian including the SOC within the framework of the density functional theory (DFT). This approach gives results with almost perfect agreement with the exact MCA energy defined as the difference of the total energies of the interacting system obtained in self-consistent-field DFT calculations (see, e.g., Refs. [25–27]).

*mcinal@ichf.edu.pl

Note that the application of the FT in the calculations of the MCA energy is not limited to layered structures since, in fact, it is valid for any magnetic system.

The MCA energy can also be determined within the perturbation theory (PT), in the second order for layered structures, with the formula proposed by Bruno [28]; its derivation and alternative forms are also discussed in Refs. [1,29] as well as the Appendix C of Ref. [30]. The perturbation formula is often used to investigate how the MCA is affected by electron states of various symmetries [27,29,31–36] and to decompose the MCA energy into terms coming from different pairs of atomic layers [6,35]. In particular, the PT formula for the MCA energy, combined with a realistic tight-binding (TB) model, was used to reveal the above-mentioned mechanism of the MCA oscillations versus Co and Pd thicknesses [3,7,8] due to specific pairs of quantum-well d states. The use of TB models, though giving a less accurate description of electronic structure, allows for reliable investigating MCA, using both the FT and the PT, for much larger systems than in the DFT approach where calculation of the small MCA energies, with typical values of 0.1–1 meV per surface atom, can become computationally demanding due to the system size (see, e.g., Refs. [1,6,8,37–40].

Alternatively, the MCA energy of a layered system can be expressed as half the difference of the total SOC energies for two magnetization directions. Although the SOC energies are found with the eigenstates of the full Hamiltonian including the SOC, this method does not reproduce exactly the MCA energy obtained with the FT using the energies of these states. In fact, the derivation of the alternative formula for the MCA energy is based, in fact, on the PT representation of this energy [41]. The expression of the MCA energy as half the SOC energy is particularly useful for defining the contributions of different atoms or atomic layers to the MCA energy as it is implemented in some DFT codes, like the Vienna *ab initio* simulation package (VASP) [42–44]. However, it should be noted that such a spatial decomposition of the MCA energy is not unique since a different pattern of its layer-resolved contributions is obtained with the method based on the layer-projected density of states (DOS) [6].

The form of the usually applied second-order PT expression for the MCA energy [1,27–29,32,45], given by a sum of interband contributions, coming from pairs of occupied and unoccupied electron states, has recently been reexamined [6]. It has been shown that the second-order intraband terms, coming from individual electron states with energies very close to the Fermi energy, must also be included. Since the intraband terms vanish in the presence of the inversion symmetry this extension is relevant only for systems without the inversion symmetry. In fact, the inclusion of the intraband terms is crucial for such systems as it was demonstrated for Co/Pd bilayers where the net intraband and interband contributions to the MCA energy are of similar magnitude though have the opposite signs so that they largely cancel out. The intraband terms of the MCA energy have also been identified, in a system-specific form, for a simple model of a heavy-metal/ferromagnetic-metal bilayer represented as a two-dimensional square lattice and described with a one-band TB model including the interfacial SOC in the Rashba-type form [46].

The presence of the intraband term of the MCA energy for an arbitrary layered system has been previously established using the PT expansion of the free energy at finite temperature T [6,9,47]. However, such a formal derivation of the PT formula for the MCA energy does not provide a clear picture of the physical mechanism of how the MCA intraband term arises. In this paper, the origin of this term is investigated in depth. By considering the band energy of the perturbed system in its ground state (i.e., at $T = 0$) it is examined how its second-order intraband term composed of squares of the first-order corrections to electron energies is related to the changes of the Fermi surface (FS) due to the SOC perturbation. As a result, the form of the intraband contributions is explained and a simple graphical interpretation of these contributions is given. In addition, it is investigated whether the expression for the MCA energy with half the SOC energy, previously derived [41] from the PT formula for the MCA energy without intraband terms, is also valid for systems without the inversion symmetry where intraband terms need to be included in this formula.

These theoretical findings are discussed in Sec. II, together with the plots of the FS sheets for an exemplary Co/Pd bilayer system, while more details are given in Appendixes A and B, the latter including an alternative derivation of the MCA intraband term at $T = 0$. The theoretical discussion is further supported in Sec. III by the results of the numerical calculations of the MCA energy, and its intraband and interband terms for a few selected Co-based layered systems (films, bilayers, and trilayers), with and without the inversion symmetry. A set of conclusions, regarding the present results and their relation to some previous work on the MCA and the magnetic damping due to the SOC, is formulated in Sec. IV.

II. THEORY

A. Magnetocrystalline anisotropy: Force theorem, perturbation theory, and intraband terms

The energy E of a thin film including a ferromagnetic layer depends on the direction $\hat{\mathbf{M}}$ of its magnetization. The resultant magnetic anisotropy energy has two terms: the shape anisotropy energy due to the magnetic dipole-dipole interaction, favoring the in-plane magnetization direction, and the MCA energy which originates from the SOC of both ferromagnetic and nonmagnetic layers. The spin-orbit interaction

$$H_{\mathrm{SO}} = \sum_{lj} \xi_l \mathbf{L}(\mathbf{r} - \mathbf{R}_{lj}) \cdot \mathbf{S} = \sum_{l} H_{\mathrm{SO}}^{(l)} \tag{1}$$

depends on the spin $\mathbf{S}$ of an electron and its orbital angular momentum $\mathbf{L}$ with respect to different atoms j located at the positions $\mathbf{R}_{lj}$ in each atomic layer l while the SOC constants ξ_l determine the strength of this interaction. According to the FT [23], the MCA energy of a film with cubic structure and the (001) or (111) surface at zero temperature can be expressed as the difference $E_{\mathrm{b}}(\hat{\mathbf{M}}_{\perp}) - E_{\mathrm{b}}(\hat{\mathbf{M}}_{\parallel})$ of the system band energies, i.e., the total energies of the occupied (occ) bands

$$E_{\mathrm{b}} = \frac{1}{\Omega_{\mathrm{2D}}} \int d\mathbf{k} \sum_{m}^{\mathrm{occ}} \epsilon_m(\mathbf{k}) \tag{2}$$

for the magnetization direction $\hat{\mathbf{M}}_\perp$ perpendicular to the film surface (along the z axis) and the in-plane magnetization $\hat{\mathbf{M}}_\parallel$ (along the x or y axes). The electron energies $\epsilon_m(\mathbf{k})$, labeled with the two-dimensional wave vector $\mathbf{k}$ and the band index m, are the energies of the eigenstates $|m\mathbf{k}\rangle$ of the perturbed Hamiltonian $H + H_{\rm SO}$ where H denotes the one-electron Hamiltonian in the absence of the SOC (in fact, this Hamiltonian describes the noninteracting Kohn-Sham system which has the total energy $E_{\rm b}$ and represents the real interacting system within the DFT). The dependence of the band energy $E_{\rm b}$ on the magnetization direction $\hat{\mathbf{M}}$ in a ferromagnetic system arises due to the fact that, although the spin-orbit interaction operator $H_{\rm SO}$ is fixed (independent of $\hat{\mathbf{M}}$), its matrix elements depend on this direction [48] for the spin-state basis $|\sigma\rangle$ ($\sigma = \uparrow, \downarrow$) corresponding to the spin quantization axis ζ along $\hat{\mathbf{M}}$ because the spin operator $\mathbf{S}$ is then represented as $(S_\xi, S_\eta, S_\zeta) = \frac{1}{2}\hbar(\sigma_1, \sigma_2, \sigma_3)$ with the Pauli matrices in the rotated frame of reference $O\xi\eta\zeta$ [1,6]; $\hbar$ is the Planck constant.

In numerical calculations, the integrals $(1/\Omega_{\rm 2D})\int d\mathbf{k}$ over the two-dimensional (2D) Brillouin zone (BZ) of the area $\Omega_{\rm 2D}$ are replaced with the finite sums $(1/N_{\rm 2D})\sum_{\mathbf{k}}$ over a grid of $N_{\rm 2D}$ discrete $\mathbf{k}$ points which can also be viewed as imposing periodic boundary conditions with $N_{\rm 2D}$ primitive unit cells in each atomic plane. The number of $\mathbf{k}$ points required for convergence of the MCA energy can be reduced [9] by considering the system of electrons with energies $\epsilon = \epsilon_m(\mathbf{k})$ at finite temperature T and using the Fermi-Dirac function $f(\epsilon) = 1/\{1 + \exp[(\epsilon - \epsilon_{\rm F})/k_{\rm B}T]\}$ for the occupation numbers of electron states; $\epsilon_{\rm F}$ is the Fermi energy (chemical potential) and $k_{\rm B}$ is the Boltzmann constant. Finite temperature T is introduced here mainly as a computational tool used for smearing the energy levels while other temperature-dependent effects, like spin waves and the resulting reduction of the saturation magnetization $M_{\rm s}$, are not accounted for. Alternatively, the convergence can be improved with other smearing methods, in particular, the Methfessel-Paxton approximation of the step-like occupation factor at zero temperature [49].

At finite temperature T, the MCA energy defined within the FT approach is expressed with the free energy $F = E_{\rm b} - TS$ of the system with the band energy $E_{\rm b}$ and the entropy S:

$$E_{\rm MCA} = E^{\rm FT}_{\rm MCA} = F(\hat{\mathbf{M}}_\perp) - F(\hat{\mathbf{M}}_\parallel). \tag{3}$$

This corresponds to describing the system in the canonical ensemble, with the fixed number of electrons

$$N = \frac{1}{\Omega_{\rm 2D}}\int d\mathbf{k}\sum_m f[\epsilon_m(\mathbf{k})] \tag{4}$$

while the Fermi energy $\epsilon_{\rm F} = \epsilon_{\rm F}(\hat{\mathbf{M}})$ found from the condition (4) depends on the magnetization direction $\hat{\mathbf{M}}$. Further, it is convenient to represent the free energy

$$F(\hat{\mathbf{M}}) = \Omega + \epsilon_{\rm F}N \tag{5}$$

with the grand potential [50]

$$\Omega(\hat{\mathbf{M}}) = \frac{1}{\Omega_{\rm 2D}}\int d\mathbf{k}\sum_m g[\epsilon_m(\mathbf{k})], \tag{6}$$

defined with the function $g(\epsilon) = -k_{\rm B}T\ln\{1 + \exp[(\epsilon_{\rm F} - \epsilon)/k_{\rm B}T]\}$ [51] while still describing the system in the canonical ensemble. For layered systems with one atom per primitive unit cell, the above formulas define the MCA energy and other respective quantities per one surface atom. Note that the band energy $E_{\rm b}$ is also replaced with a free energy F in other smearing methods; however, the corresponding form of F is different, specific to the smearing method applied [43,44].

For each electron state $|m\mathbf{k}\rangle = |n\mathbf{k}\sigma\rangle^{\rm per}$ perturbed by the SOC, its energy can be expanded up to the second order in $H_{\rm so}$ as follows:

$$\epsilon_m = \epsilon^{\rm per}_{n\sigma} = \epsilon_{n\sigma} + \delta\epsilon_{n\sigma}, \tag{7}$$

where $\epsilon_{n\sigma} = \epsilon_{n\sigma}(\mathbf{k})$ is the energy of the unperturbed state $|n\sigma\mathbf{k}\rangle$ with spin σ ($\uparrow$ or $\downarrow$), band index n, and the wave vector $\mathbf{k}$ while the change of the unperturbed energy due to the SOC

$$\delta\epsilon_{n\sigma} = \epsilon^{(1)}_{n\sigma} + \epsilon^{(2)}_{n\sigma} \tag{8}$$

includes the first- and second-order corrections

$$\epsilon^{(1)}_{n\sigma} = \langle n\mathbf{k}\sigma|H_{\rm SO}|n\mathbf{k}\sigma\rangle, \tag{9}$$

$$\epsilon^{(2)}_{n\sigma} = \sum_{n'\sigma'\neq n\sigma}\frac{|\langle n'\mathbf{k}\sigma'|H_{\rm SO}|n\mathbf{k}\sigma\rangle|^2}{\epsilon_{n\sigma}(\mathbf{k}) - \epsilon_{n'\sigma'}(\mathbf{k})}. \tag{10}$$

This leads to the corresponding expansions of the free energy $F = F_0 + F^{(1)} + F^{(2)}$ and the grand potential $\Omega = \Omega_0 + \Omega^{(1)} + \Omega^{(2)}$ where $F_0 = \Omega_0 + \epsilon_0 N$, $F^{(1)} = \Omega^{(1)}$, and $F^{(2)} = \Omega^{(2)}$ (see the Appendix in Ref. [6]). For systems with the inversion symmetry, the electron energy term $\epsilon^{(1)}_{n\sigma}$ linear in the SOC vanishes for each state $n\sigma$ and so does the respective correction $F^{(1)}$ to the free energy. However, the first-order term $F^{(1)}$ vanishes also in the absence of the inversion symmetry for systems with collinear magnetic structure, due to cancellation of possibly finite $\mathbf{k}$ and $-\mathbf{k}$ contributions (for systems with noncollinear magnetic structures this term can be finite which leads to the Dzyaloshinskii-Moriya interaction [52]). Indeed, the matrix elements $\langle n\mathbf{k}\sigma|H_{\rm so}|n\mathbf{k}\sigma\rangle$ have opposite values for $\mathbf{k}$ and $-\mathbf{k}$ since for each eigenstate $|n\mathbf{k}\sigma\rangle$ of the unperturbed Hamiltonian H with the wave function $\psi^\sigma_{n\mathbf{k}}(\mathbf{r})$ there is another eigenstate $|n, -\mathbf{k}, \sigma\rangle$ with the same energy and the wave function $\psi^\sigma_{n,-\mathbf{k}}(\mathbf{r}) = [\psi^\sigma_{n\mathbf{k}}(\mathbf{r})]^*$ which gives the opposite expectation value of $\mathbf{L}$ (see, e.g., Ref. [9]). Thus, for layered systems with ferromagnetic layers, the dominant correction to the free energy is of the second order in the SOC [6,9,47]:

$$F^{(2)}(\hat{\mathbf{M}}) = \Omega^{(2)}(\hat{\mathbf{M}}) = \frac{1}{2}\frac{1}{\Omega_{\rm 2D}}\int d\mathbf{k} \times \sum_{n\sigma}\sum_{n'\sigma'}\frac{f_0(\epsilon_{n\sigma}(\mathbf{k})) - f_0(\epsilon_{n'\sigma'}(\mathbf{k}))}{\epsilon_{n\sigma}(\mathbf{k}) - \epsilon_{n'\sigma'}(\mathbf{k})} \times |\langle n'\mathbf{k}\sigma'|H_{\rm SO}|n\mathbf{k}\sigma\rangle|^2, \tag{11}$$

where the occupation factors $f_0(\epsilon_{n\sigma}) = f(\epsilon_{n\sigma}; \epsilon_{\rm F} = \epsilon_{\rm F0})$ correspond to the unperturbed system with the Fermi energy $\epsilon_{\rm F0}$. As a result, the PT formula for the MCA energy of thin films takes the form

$$E_{\rm MCA} = E^{\rm PT}_{\rm MCA} = F^{(2)}(\hat{\mathbf{M}}_\perp) - F^{(2)}(\hat{\mathbf{M}}_\parallel). \tag{12}$$

The expression (11) for $F^{(2)}$ includes both the off-diagonal (interband) contributions $n\sigma \neq n'\sigma'$ coming from

the second-order corrections $\epsilon_{n\sigma}^{(2)}$ to electron energies as well as the diagonal (intraband) terms $n\sigma = n'\sigma'$, proportional to $f_0'(\epsilon_{n\sigma})|\epsilon_{n\sigma}^{(1)}|^2$, which comprise the squared moduli of the first-order corrections $\epsilon_{n\sigma}^{(1)}$ or rather their squares $(\epsilon_{n\sigma}^{(1)})^2$ since the diagonal elements of the Hermitian operator H_{SO} are real. The latter contributions arise from the quadratic term in the power-series expansion of the function $g(\epsilon = \epsilon_{n\sigma} + \delta\epsilon_{n\sigma}) = g_0(\epsilon = \epsilon_{n\sigma} + \delta\epsilon_{n\sigma} - \delta\epsilon_{\mathrm{F}})$ expressed with $\delta\epsilon_{n\sigma}$, $\delta\epsilon_{\mathrm{F}} = \epsilon_{\mathrm{F}} - \epsilon_{\mathrm{F}0}$ and the function $g_0(\epsilon) = g(\epsilon; \epsilon_{\mathrm{F}} = \epsilon_{\mathrm{F}0})$, which corresponds to the unperturbed system and has the derivatives $g_0'(\epsilon) = f_0(\epsilon)$ and $g_0''(\epsilon) = f_0'(\epsilon)$,

Thus, the second-order correction to the free energy

$$F^{(2)} = F_{\mathrm{inter}}^{(2)} + F_{\mathrm{intra}}^{(2)} \tag{13}$$

comprises both the interband term

$$\begin{aligned} F_{\mathrm{inter}}^{(2)} &= \frac{1}{\Omega_{\mathrm{2D}}} \int d\mathbf{k} \sum_{n\sigma} f_0(\epsilon_{n\sigma}) \epsilon_{n\sigma}^{(2)} \\ &= \frac{1}{2} \frac{1}{\Omega_{\mathrm{2D}}} \int d\mathbf{k} \sum_{n\sigma} \sum_{n'\sigma' \neq n\sigma} \frac{f_0(\epsilon_{n\sigma}) - f_0(\epsilon_{n'\sigma'})}{\epsilon_{n\sigma} - \epsilon_{n'\sigma'}} \\ &\quad \times |\langle n'\mathbf{k}\sigma' | H_{\mathrm{SO}} | n\mathbf{k}\sigma \rangle|^2 \end{aligned} \tag{14}$$

and the intraband term

$$\begin{aligned} F_{\mathrm{intra}}^{(2)} &= \frac{1}{2} \frac{1}{\Omega_{\mathrm{2D}}} \int d\mathbf{k} \sum_{n\sigma} f_0'(\epsilon_{n\sigma}) \left(\epsilon_{n\sigma}^{(1)}\right)^2 \\ &= \frac{1}{2} \frac{1}{\Omega_{\mathrm{2D}}} \int d\mathbf{k} \sum_{n\sigma} f_0'(\epsilon_{n\sigma}) |\langle n\mathbf{k}\sigma | H_{\mathrm{SO}} | n\mathbf{k}\sigma \rangle|^2 . \end{aligned} \tag{15}$$

Note that the intraband term $F_{\mathrm{intra}}^{(2)}$ is nonpositive since the derivative $f_0'(\epsilon_{n\sigma})$ is negative for any energy $\epsilon_{n\sigma}$; this term can be equal to 0 for a specific magnetization direction even in the absence of the inversion symmetry and vanishes for any systems that possess this symmetry (cf. Sec. III).

The detailed derivation of Eq. (11) is given in the Appendix of Ref. [6]. The same expression for $F^{(2)} = \Omega^{(2)}$ can be obtained from the Dyson expansion for the perturbed Green function [9] so that the intraband contributions are automatically included in the MCA energy if it is calculated using solely the Green functions, instead electron states and their energies, as it is done, e.g., in Refs. [35,38,53].

The formula (11) remains valid if there are degenerate states $|n\mathbf{k}\sigma\rangle$ at some $\mathbf{k}$ points (in particular, at high-symmetry points and lines), though the decomposition of their contributions into intraband and interband terms is then not unique due to different possible choices of orthonormal eigenstates forming a basis in a degenerate subspace of the Hamiltonian H. However, as it is demonstrated in Ref. [6], the subsum of all (both intraband and interband) second-order contributions calculated within a degenerate subspace of dimension M,

$$\sum_{i,j=1}^{M} f_0'(\epsilon_{n_j\sigma}) |\langle n_i\mathbf{k}\sigma | H_{\mathrm{SO}} | n_j\mathbf{k}\sigma \rangle|^2, \tag{16}$$

does not depend on the choice of its M orthonormal basis states $|n_j\mathbf{k}\sigma\rangle$ $(j = 1, \ldots, M)$ of the same spin σ and with the equal energies $\epsilon_{n_i\sigma}(\mathbf{k}) = \epsilon_{n_j\sigma}(\mathbf{k})$; note that the factor $f_0'(\epsilon_{n_j\sigma})$ is the same for all these contributions. This subsum is reduced to the sum of the intraband contributions from this subspace, a part of $F_{\mathrm{intra}}^{(2)}$ defined in Eq. (15), if the chosen basis states diagonalize the matrix of the H_{SO} perturbation operator within the subspace. Thus, Eq. (16) uniquely defines the internal contribution of a degenerate subspace to $F^{(2)}$ so that there is no need for the mentioned diagonalization although it is formally required in the PT approach in the case of degenerate states. This is even more so because the sum of the remaining interband contributions involving this degenerate subspace, which come from its orthonormal basis states coupled to all other states (from outside the subspace), is also invariant with respect to the choice of this basis [6]. In view of these findings, the ambiguity in the decomposition of $F^{(2)}$ can be readily avoided if the full internal contribution from each degenerate subspace, given by Eq. (16), is included solely into the intraband term $F_{\mathrm{intra}}^{(2)}$ so that this term is then uniquely defined.

Nevertheless, such a modification of the intraband term leads to its only slight adjustment since the internal contributions from the degenerate subspaces effectively come from a discrete set of $\mathbf{k}$ points and their immediate neighborhoods (the later at finite T) while the intraband contributions to $F^{(2)}$ from nondegenerate states come from the curves in the two-dimensional BZ representing different sheets of the FS (see the next section) and the regions in their immediate vicinity, also due to finite T. Indeed, the degenerate subspaces that can give a significant internal contribution to $F^{(2)}$ must have the energies very close to the Fermi energy, not farther than a few $k_{\mathrm{B}}T$ from ϵ_{F}, due to the presence of the factor $f_0'(\epsilon_{n_j\sigma})$ in Eq. (16). As a result, if two or more electron energy bands are degenerate along a whole high-symmetry line the internal contribution of the corresponding degenerate subspace to $F^{(2)}$ is non-negligible only in a very small region around the point on this high-symmetry line where the degenerate bands cross the Fermi energy. A similar conclusion could be drawn if there was an accidental degeneracy of two energy bands outside the high-symmetry lines. In this case, there would be contributions from the respective degenerate subspace only at and in the very close vicinity of the general $\mathbf{k}$ point (or a few such points) where the energy of the crossing bands is equal to the Fermi energy.

The presence of the contributions from degenerate subspaces is even more limited in layered systems without the inversion symmetry which have a cubic structure and the (001) surface, like the Co/X bilayers investigated in Sec. III. Indeed, in such systems, there are no degenerate states even on the high-symmetry lines, except at their ends which are the high-symmetry points, $\overline{\Gamma}$, $\overline{X}$, and $\overline{M}$, where such states are still present. To show this, let us consider the group $G_{\mathbf{k}}$ of the wave vector $\mathbf{k}$ which includes all the symmetry operations that transform $\mathbf{k}$ to itself or an equivalent wave vector $\mathbf{k} + \mathbf{G}$ in the BZ where $\mathbf{G}$ is a reciprocal lattice vector [54]. For a $\mathbf{k}$ point inside one of the three high-symmetry lines, $\overline{\Gamma}$–$\overline{M}$, $\overline{\Gamma}$–$\overline{X}$, and $\overline{X}$–$\overline{M}$ (excluding their ends), the respective symmetry group $G_{\mathbf{k}}$ has only two elements, the identity transformation E and the reflection σ_v in the plane perpendicular to the film surface and parallel to the considered high-symmetry line. Such a group has two irreducible representations, both one dimensional, since the sum of the squares of the dimensions

of all (inequivalent) irreducible representations of a group is equal to the number of its elements [54]. Thus, for the considered system, the electron states with the wave vectors at the high-symmetry lines are nondegenerate, apart from the high-symmetry points at the ends of these lines where the respective symmetry groups $G_{\mathbf{k}}$ include more elements and have both one- and two-dimensional irreducible representations. However, even the degenerate subspaces at the high-symmetry points can give negligible internal contributions to $F^{(2)}$ given in Eq. (16) if their energies are not very close to the Fermi energy.

B. Origin of intraband term of MCA energy: Perturbation expansion of system band energy at $T = 0$

While the finite-temperature formulation is convenient in the numerical calculations since the smearing of electron energies provides better convergence of the calculated MCA energy (cf. Sec. III B below) the physical origin of its intraband term can be more efficiently investigated by considering the system in its ground state, i.e., at zero temperature. It is found that the intraband terms, which are finite for systems without the inversion symmetry, are preserved in the $T \to 0$ limit

$$\lim_{T\to 0} F^{(2)}_{\text{intra}} = -\frac{1}{2}\frac{1}{\Omega_{2\text{D}}}\sum_{n\sigma}\int d\mathbf{k}\,\delta(\epsilon_{n\sigma}(\mathbf{k}) - \epsilon_{\text{F}0})\left(\epsilon^{(1)}_{n\sigma}\right)^2, \quad (17)$$

where the derivative $f_0'(\epsilon_{n\sigma})$ becomes the negative of the Dirac delta function $\delta(\epsilon_{n\sigma}(\mathbf{k}) - \epsilon_{\text{F}0})$; the order of the two sums in this formula has been changed for the sake of the following discussion. If the matrix element $\epsilon^{(1)}_{n\sigma} = \langle n\mathbf{k}\sigma|H_{\text{SO}}|n\mathbf{k}\sigma\rangle$, or rather its square, was assumed to be constant throughout the BZ the intraband term of $F^{(2)}$ in the $T \to 0$ limit would be proportional to the DOS $n(\epsilon) = (1/\Omega_{2\text{D}})\int d\mathbf{k}\sum_{n\sigma}\delta(\epsilon_{n\sigma}(\mathbf{k}) - \epsilon)$ at the Fermi level $\epsilon = \epsilon_{\text{F}0}$, multiplied by the constant $(\epsilon^{(1)}_{n\sigma})^2$, a result similar to the one obtained for a bilayer system in a simple one-band TB model [46]. However, such an assumption does not hold for real systems described with the DFT or a multiple-orbital TB model since the matrix element of H_{SO} that defines $\epsilon^{(1)}_{n\sigma}$, Eq. (9), strongly depends on the symmetry of electron states $|n\mathbf{k}\sigma\rangle$ as well as the wave vector $\mathbf{k}$.

The function $\delta(\epsilon_{n\sigma}(\mathbf{k}) - \epsilon_{\text{F}0})$ vanishes outside the set of $\mathbf{k} = \mathbf{k}_s$ points that satisfy the relation $\epsilon_{n\sigma}(\mathbf{k}) = \epsilon_{\text{F}0}$ and thus form a curve in the two-dimensional BZ. This curve is the sheet $\mathcal{C}_{n\sigma}$ of the FS for band n of spin σ in the unperturbed system; for simplicity, the single symbol $\mathcal{C}_{n\sigma}$ is used here even if the relation $\epsilon_{n\sigma}(\mathbf{k}) = \epsilon_{\text{F}0}$ defines a set a few separate curves which could be alternatively treated as separate FS sheets. At each point $\mathbf{k}_s \in \mathcal{C}_{n\sigma}$, the gradient $\nabla_{\mathbf{k}}\epsilon_{n\sigma}(\mathbf{k}_s)$ is perpendicular to (the tangent of) the curve $\mathcal{C}_{n\sigma}$ so the electron energy can be expanded in the vicinity of this curve as follows:

$$\epsilon_{n\sigma}(\mathbf{k}) - \epsilon_{\text{F}0} = \nabla_{\mathbf{k}}\epsilon_{n\sigma}(\mathbf{k}_s)\cdot(\mathbf{k} - \mathbf{k}_s) = |\nabla_{\mathbf{k}}\epsilon_{n\sigma}(\mathbf{k}_s)|q_\perp. \quad (18)$$

Here, the wave vectors lie on the line perpendicular to $\mathcal{C}_{n\sigma}$ at $\mathbf{k}_s$ and are represented as $\mathbf{k} = \mathbf{k}_s + q_\perp\mathbf{e}_\perp$ where $\mathbf{e}_\perp = \nabla_{\mathbf{k}}\epsilon_{n\sigma}(\mathbf{k}_s)/|\nabla_{\mathbf{k}}\epsilon_{n\sigma}(\mathbf{k}_s)|$ is the unit vector along the gradient direction. With this expansion, the Dirac delta function becomes $\delta(\epsilon_{n\sigma}(\mathbf{k}) - \epsilon_{\text{F}0}) = \delta(q_\perp)/|\nabla_{\mathbf{k}}\epsilon_{n\sigma}(\mathbf{k}_s)|$ so, after integration over $q_\perp$, the two-dimensional integral over $\mathbf{k}$ in Eq. (17) is reduced to the line integral along the curve $\mathcal{C}_{n\sigma}$, i.e., the FS sheet of band $n\sigma$. As a result, in the $T \to 0$ limit, the intraband contribution to $F^{(2)}$ is given by the sum of contributions from different FS sheets:

$$\begin{aligned}\lim_{T\to 0} F^{(2)}_{\text{intra}} &= -\frac{1}{2}\frac{1}{\Omega_{2\text{D}}}\sum_{n\sigma}\int_{\mathcal{C}_{n\sigma}} ds\,\frac{|\langle n\mathbf{k}_s\sigma|H_{\text{SO}}|n\mathbf{k}_s\sigma\rangle|^2}{|\nabla_{\mathbf{k}}\epsilon_{n\sigma}(\mathbf{k}_s)|}\\ &= -\frac{1}{2}\frac{1}{\Omega_{2\text{D}}}\sum_{n\sigma}\int_{\mathcal{C}_{n\sigma}} ds\,\frac{\left[\epsilon^{(1)}_{n\sigma}(\mathbf{k}_s)\right]^2}{|\nabla_{\mathbf{k}}\epsilon_{n\sigma}(\mathbf{k}_s)|}, \end{aligned} \quad (19)$$

where $ds = |d\mathbf{k}_s|$. This contribution accompanies the interband term of $F^{(2)}$ at the $T \to 0$ limit which takes the usual form

$$\lim_{T\to 0} F^{(2)}_{\text{inter}} = \frac{1}{\Omega_{2\text{D}}}\int d\mathbf{k}\sum_{n\sigma}^{\text{occ}}\sum_{n'\sigma'}^{\text{unocc}}\frac{|\langle n'\mathbf{k}\sigma'|H_{\text{so}}|n\mathbf{k}\sigma\rangle|^2}{\epsilon_{n\sigma}(\mathbf{k}) - \epsilon_{n'\sigma'}(\mathbf{k})}, \quad (20)$$

including the sums over occupied (occ) and unoccupied (unocc) electron states. The latter term is equal to the contribution to the perturbed band energy

$$E^{(2)}_{\text{b}} = \frac{1}{\Omega_{2\text{D}}}\int d\mathbf{k}\sum_{n\sigma}^{\text{occ}}\epsilon^{(2)}_{n\sigma}(\mathbf{k}) \quad (21)$$

from the second-order corrections $\epsilon^{(2)}_{n\sigma}$ to electron energies.

Thus, the expression for the MCA energy obtained with Eq. (12) in the $T \to 0$ limit differs from the usual second-order PT formula $E^{(2)}_{\text{b}}(\hat{\mathbf{M}}_\perp) - E^{(2)}_{\text{b}}(\hat{\mathbf{M}}_\parallel)$ for E_{MCA} at $T = 0$ where the intraband terms are not present [1,28,29]. This discrepancy originates from the implicit assumption, made in the derivation of the latter formula, that all occupied unperturbed electron states remain occupied after the SOC perturbation is introduced so that the band energy, Eq. (2), calculated with $\epsilon_m = \epsilon_{n\sigma} + \epsilon^{(1)}_{n\sigma} + \epsilon^{(2)}_{n\sigma}$ is equal to $E^{(0)}_{\text{b}} + E^{(1)}_{\text{b}} + E^{(2)}_{\text{b}} = E^{(0)}_{\text{b}} + E^{(2)}_{\text{b}}$ where $E^{(0)}_{\text{b}} = (1/\Omega_{2\text{D}})\int d\mathbf{k}\sum_{n\sigma}^{\text{occ}}\epsilon_{n\sigma}(\mathbf{k})$ is the unperturbed band energy and the first-order correction $E^{(1)}_{\text{b}} = (1/\Omega_{2\text{D}})\int d\mathbf{k}\sum_{n\sigma}^{\text{occ}}\epsilon^{(1)}_{n\sigma}(\mathbf{k})$ vanishes due to cancellation of $\mathbf{k}$ and $-\mathbf{k}$ contributions $[\epsilon^{(1)}_{n\sigma}(-\mathbf{k}) = -\epsilon^{(1)}_{n\sigma}(\mathbf{k})]$. On the other hand, no such assumption is made, or is even possible to make, in the derivation of the expression for $F^{(2)}$ at finite T as the occupations of electron states, unperturbed and perturbed, are governed by the Fermi-Dirac function with the respective Fermi energies $\epsilon_{\text{F}0}$ and ϵ_{F}.

However, this assumption is, in fact, not valid also at $T = 0$ since for metallic extended systems with continuous electron energy spectrum some of the electron states which are occupied become unoccupied upon the introduction of a perturbation and, vice versa, some unoccupied states become occupied. This concerns a fraction of states with energies very close to the Fermi level. Thus, the band energy of the perturbed system can be represented in the following way:

$$\begin{aligned}E_{\text{b}} &= \frac{1}{\Omega_{2\text{D}}}\sum_{n\sigma}\int_{\mathcal{F}_{n\sigma}} d\mathbf{k}\,\epsilon^{\text{per}}_{n\sigma}(\mathbf{k})\\ &= \frac{1}{\Omega_{2\text{D}}}\sum_{n\sigma}\int_{\mathcal{F}^{(0)}_{n\sigma}} d\mathbf{k}\,\epsilon^{\text{per}}_{n\sigma}(\mathbf{k}) + \frac{1}{\Omega_{2\text{D}}}\sum_{n\sigma}\int_{\mathcal{F}_{n\sigma}-\mathcal{F}^{(0)}_{n\sigma}} d\mathbf{k}\,\epsilon^{\text{per}}_{n\sigma}(\mathbf{k})\\ &\quad - \frac{1}{\Omega_{2\text{D}}}\sum_{n\sigma}\int_{\mathcal{F}^{(0)}_{n\sigma}-\mathcal{F}_{n\sigma}} d\mathbf{k}\,\epsilon^{\text{per}}_{n\sigma}(\mathbf{k}), \end{aligned} \quad (22)$$

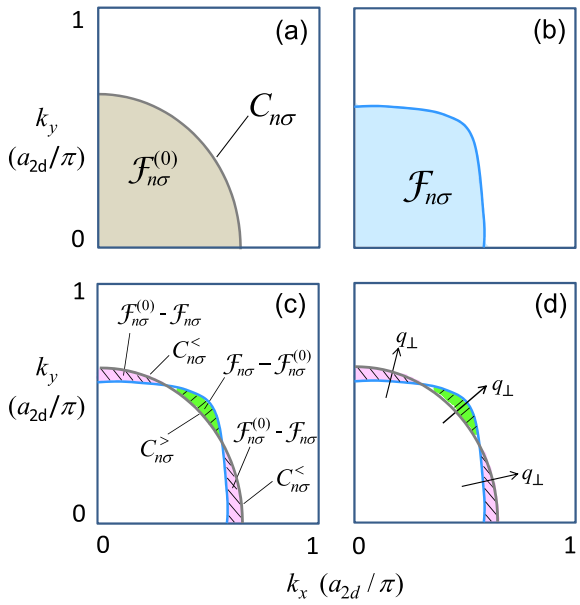

FIG. 1. (a), (b) Schematic of the sets $\mathcal{F}^{(0)}_{n\sigma}$ and $\mathcal{F}_{n\sigma}$ of $\mathbf{k}$ points with the occupied states in the energy band $n\sigma$ obtained without and with the SOC, respectively, and (c) the differences of the two sets; (a) the FS sheet $C_{n\sigma}$ for the band obtained without the SOC and (c) its parts $C^{<}_{n\sigma}$ and $C^{>}_{n\sigma}$ defined in text; (d) the $q_\perp$ axes perpendicular to the sheet curve $C_{n\sigma}$ at its three selected points. Plots are shown in a quarter of a square two-dimensional BZ.

where, in each term, there is a two-dimensional integral over $\mathbf{k}$ from the specified subsets of the BZ. The sets $\mathcal{F}^{(0)}_{n\sigma} = \{\mathbf{k} : \epsilon_{n\sigma}(\mathbf{k}) \leqslant \epsilon_{\mathrm{F}0}\}$ and $\mathcal{F}_{n\sigma} = \{\mathbf{k} : \epsilon^{\mathrm{per}}_{n\sigma}(\mathbf{k}) \leqslant \epsilon_{\mathrm{F}}\}$ are defined as the parts of the BZ with the occupied electron states from band $n\sigma$ in the unperturbed and perturbed system, respectively; the two sets and their differences are schematically depicted in Fig. 1. By representing the perturbed electron energies as

$$\epsilon^{\mathrm{per}}_{n\sigma} = \epsilon_{n\sigma} + \delta\epsilon_{n\sigma} = \epsilon_{n\sigma} - \epsilon_{\mathrm{F}0} + \delta\epsilon_{n\sigma} + \epsilon_{\mathrm{F}0}, \tag{23}$$

we can rewrite Eq. (22) as follows:

$$\begin{aligned}\Omega_{2\mathrm{D}}E_{\mathrm{b}} = &\sum_{n\sigma}\int_{\mathcal{F}^{(0)}_{n\sigma}} d\mathbf{k}(\epsilon_{n\sigma} + \delta\epsilon_{n\sigma}) \\ &+ \sum_{n\sigma}\int_{\mathcal{F}_{n\sigma}-\mathcal{F}^{(0)}_{n\sigma}} d\mathbf{k}(\epsilon_{n\sigma} - \epsilon_{\mathrm{F}0} + \delta\epsilon_{n\sigma}) \\ &- \sum_{n\sigma}\int_{\mathcal{F}^{(0)}_{n\sigma}-\mathcal{F}_{n\sigma}} d\mathbf{k}(\epsilon_{n\sigma} - \epsilon_{\mathrm{F}0} + \delta\epsilon_{n\sigma}) \\ &+ \epsilon_{\mathrm{F}0}\left[\sum_{n\sigma}\int_{\mathcal{F}_{n\sigma}-\mathcal{F}^{(0)}_{n\sigma}} d\mathbf{k}\,1 - \sum_{n\sigma}\int_{\mathcal{F}^{(0)}_{n\sigma}-\mathcal{F}_{n\sigma}} d\mathbf{k}\,1\right].\end{aligned} \tag{24}$$

The first term is equal to $E^{(0)}_{\mathrm{b}} + E^{(1)}_{\mathrm{b}} + E^{(2)}_{\mathrm{b}} = E^{(0)}_{\mathrm{b}} + E^{(2)}_{\mathrm{b}}$, multiplied by $\Omega_{2\mathrm{D}}$, where the linear term $E^{(1)}_{\mathrm{b}}$ vanishes. The expression in the square brackets in the last term also vanishes since it is equal to the difference of the numbers (multiplied by $\Omega_{2\mathrm{D}}$) of the occupied states, $\sum_{n\sigma}\int_{\mathcal{F}_{n\sigma}} d\mathbf{k}\,1$ and $\sum_{n\sigma}\int_{\mathcal{F}^{(0)}_{n\sigma}} d\mathbf{k}\,1$, in the unperturbed and perturbed systems, respectively, while both numbers are identical, equal to the fixed number N of electrons in the system.

The region $\mathcal{F}_{n\sigma} - \mathcal{F}^{(0)}_{n\sigma} = \{\mathbf{k} : \mathbf{k} \in \mathcal{F}_{n\sigma}, \mathbf{k} \notin \mathcal{F}^{(0)}_{n\sigma}\}$ in the two-dimensional BZ is determined with the relation

$$0 < \epsilon_{n\sigma}(\mathbf{k}) - \epsilon_{\mathrm{F}0} \leqslant \delta\epsilon_{\mathrm{F}} - \delta\epsilon_{n\sigma}(\mathbf{k}) \tag{25}$$

and has the shape of a narrow stripe

$$\mathcal{F}_{n\sigma} - \mathcal{F}^{(0)}_{n\sigma} = \{\mathbf{k} = \mathbf{k}_s + q_\perp\mathbf{e}_\perp : \mathbf{k}_s \in \mathcal{C}^{>}_{n\sigma}, 0 < q_\perp \leqslant w_\perp(\mathbf{k}_s)\} \tag{26}$$

attached to one side of the FS sheet curve $\mathcal{C}_{n\sigma}$, or rather its part $\mathcal{C}^{>}_{n\sigma}$ where $\delta\epsilon_{\mathrm{F}} - \delta\epsilon_{n\sigma}(\mathbf{k}_s) > 0$ [see Fig. 1(c)]. The width of this stripe

$$\begin{aligned} w_\perp(\mathbf{k}_s) &= \frac{\delta\epsilon_{\mathrm{F}} - \delta\epsilon_{n\sigma}(\mathbf{k}_s)}{|\nabla_{\mathbf{k}}\epsilon_{n\sigma}(\mathbf{k}_s)| + [\nabla_{\mathbf{k}}\delta\epsilon_{n\sigma}(\mathbf{k}_s)]_\perp} \\ &= \frac{\delta\epsilon_{\mathrm{F}} - \delta\epsilon_{n\sigma}(\mathbf{k}_s)}{|\nabla_{\mathbf{k}}\epsilon_{n\sigma}(\mathbf{k}_s)|}[1 + O(\delta\epsilon_{n\sigma})] \end{aligned} \tag{27}$$

varies with $\mathbf{k}_s \in \mathcal{C}^{>}_{n\sigma}$ and can be determined from the relation (25) using the linear expansion (18) and a similar expansion for the electron energy correction

$$\begin{aligned}\delta\epsilon_{n\sigma}(\mathbf{k}) = \delta\epsilon_{n\sigma}(\mathbf{k}_s) + \nabla_{\mathbf{k}}\delta\epsilon_{n\sigma}(\mathbf{k}_s)\cdot(\mathbf{k} - \mathbf{k}_s) = \delta\epsilon_{n\sigma}(\mathbf{k}_s) \\ + [\nabla_{\mathbf{k}}\delta\epsilon_{n\sigma}(\mathbf{k}_s)]_\perp\, q_\perp.\end{aligned} \tag{28}$$

The scalar term $[\nabla_{\mathbf{k}}\delta\epsilon_{n\sigma}(\mathbf{k}_s)]_\perp = [\nabla_{\mathbf{k}}\delta\epsilon_{n\sigma}(\mathbf{k}_s)]\cdot\mathbf{e}_\perp(\mathbf{k}_s)$, linear or quadratic in SOC (in the absence or presence of the inversion symmetry, respectively), leads to a minor correction $O(\delta\epsilon_{n\sigma})$ in the square brackets in Eq. (27) for $w_\perp$.

The two-dimensional integration over the stripe-shaped region $\mathcal{F}_{n\sigma} - \mathcal{F}^{(0)}_{n\sigma}$ in the second term of Eq. (24) can now be done in two steps, by first integrating over $q_\perp$ across the stripe, i.e., over the interval $0 < q_\perp < w_\perp(\mathbf{k}_s)$ at each point $\mathbf{k}_s \in \mathcal{C}^{>}_{n\sigma}$, followed by the line integral along the curve $\mathcal{C}^{>}_{n\sigma}$. The integral over $q_\perp$ of the function $\epsilon_{n\sigma}(\mathbf{k}) - \epsilon_{\mathrm{F}0} + \delta\epsilon_{n\sigma}(\mathbf{k})$ expressed with Eqs. (18) and (28) is equal to

$$\begin{aligned}\frac{1}{2}|\nabla_{\mathbf{k}}\epsilon_{n\sigma}|w^2_\perp + w_\perp\delta\epsilon_{n\sigma} &= \frac{1}{|\nabla_{\mathbf{k}}\epsilon_{n\sigma}|}\left[\frac{1}{2}(\delta\epsilon_{\mathrm{F}} - \delta\epsilon_{n\sigma})^2\right. \\ &\quad \left. + (\delta\epsilon_{\mathrm{F}} - \delta\epsilon_{n\sigma})\delta\epsilon_{n\sigma}\right] \\ &= \frac{1}{2|\nabla_{\mathbf{k}}\epsilon_{n\sigma}|}\left[(\delta\epsilon_{\mathrm{F}})^2 - (\delta\epsilon_{n\sigma})^2\right],\end{aligned} \tag{29}$$

where all quantities are calculated at the points $\mathbf{k} = \mathbf{k}_s$ from $\mathcal{C}^{>}_{n\sigma}$ and the terms including $[\nabla_{\mathbf{k}}\delta\epsilon_{n\sigma}]_\perp$ are neglected since they are of the third or higher orders in the SOC.

A similar calculation can be done for the region $\mathcal{F}^{(0)}_{n\sigma} - \mathcal{F}_{n\sigma} = \{\mathbf{k} : \mathbf{k} \in \mathcal{F}^{(0)}_{n\sigma}, \mathbf{k} \notin \mathcal{F}_{n\sigma}\}$ including the wave vectors that satisfy the relation

$$\delta\epsilon_{\mathrm{F}} - \delta\epsilon_{n\sigma}(\mathbf{k}) < \epsilon_{n\sigma}(\mathbf{k}) - \epsilon_{\mathrm{F}0} \leqslant 0. \tag{30}$$

This region is also a narrow stripe

$$\mathcal{F}^{(0)}_{n\sigma} - \mathcal{F}_{n\sigma} = \{\mathbf{k} = \mathbf{k}_s + q_\perp\mathbf{e}_\perp : \mathbf{k}_s \in \mathcal{C}^{<}_{n\sigma}, w_\perp(\mathbf{k}_s) < q_\perp \leqslant 0\} \tag{31}$$

attached to the part $\mathcal{C}^{<}_{n\sigma}$ of the the FS sheet $\mathcal{C}_{n\sigma}$ where $\delta\epsilon_{\mathrm{F}} - \delta\epsilon_{n\sigma}(\mathbf{k}_s) < 0$ [see Fig. 1(c)]. The width of the stripe is equal to

$|w_\perp(\mathbf{k}_s)| = -w_\perp(\mathbf{k}_s)$, with $w_\perp$ defined by the same formula as in Eq. (27). The integration of $\epsilon_{n\sigma}(\mathbf{k}) - \epsilon_{\mathrm{F}0} + \delta\epsilon_{n\sigma}(\mathbf{k})$ over $w_\perp < q_\perp \leqslant 0$ then gives

$$-\frac{1}{2}|\nabla_{\mathbf{k}}\epsilon_{n\sigma}|w_\perp^2 - w_\perp\delta\epsilon_{n\sigma} = -\frac{1}{2|\nabla_{\mathbf{k}}\epsilon_{n\sigma}|}\left[(\delta\epsilon_{\mathrm{F}})^2 - (\delta\epsilon_{n\sigma})^2\right], \tag{32}$$

where all quantities are calculated at the $\mathbf{k} = \mathbf{k}_s$ points from $\mathcal{C}^<_{n\sigma}$. The obtained formula is identical to the result for the $\mathcal{F}_{n\sigma} - \mathcal{F}^{(0)}_{n\sigma}$ set, Eq. (29), except for the difference in sign. The formulas for the contributions from the $\mathcal{F}_{n\sigma} - \mathcal{F}^{(0)}_{n\sigma}$ and $\mathcal{F}^{(0)}_{n\sigma} - \mathcal{F}_{n\sigma}$ sets can be easily interpreted in a geometrical way as shown in in Fig. 2 where these contributions are represented as the difference of the areas of two triangles or the area of a trapezoid, respectively.

Note that, for some of the bands, the set $\mathcal{F}^{(0)}_{n\sigma} - \mathcal{F}_{n\sigma}$ can be empty and will then not contribute in Eq. (24). This happens if $\delta\epsilon_{\mathrm{F}} - \delta\epsilon_{n\sigma}(\mathbf{k}_s)$ is positive at every point $\mathbf{k}_s \in \mathcal{C}_{n\sigma}$ so that the FS sheet of band $n\sigma$ has no $\mathcal{C}^<_{n\sigma}$ part while a finite contribution to E_{b} comes from the nonempty set $\mathcal{F}_{n\sigma} - \mathcal{F}^{(0)}_{n\sigma}$ associated with $\mathcal{C}^>_{n\sigma} = \mathcal{C}_{n\sigma}$. In the opposite case, with negative $\delta\epsilon_{\mathrm{F}} - \delta\epsilon_{n\sigma}(\mathbf{k}_s)$ at each $\mathbf{k}_s \in \mathcal{C}_{n\sigma}$, it is the set $\mathcal{F}^{(0)}_{n\sigma} - \mathcal{F}_{n\sigma}$ that contributes while the other set is empty. There is also the third possibility where both the sets exist for a specific band $n\sigma$ since $\delta\epsilon_{\mathrm{F}} - \delta\epsilon_{n\sigma}(\mathbf{k}_s)$ has different signs in different parts of the sheet $\mathcal{C}_{n\sigma}$ as illustrated in Fig. 1(c).

In a general case, with contributions from both these sets included in Eq. (24), the third term in this equation comes with the negative sign, so that its second and third terms, coming from the $\mathcal{F}_{n\sigma} - \mathcal{F}^{(0)}_{n\sigma}$ and $\mathcal{F}^{(0)}_{n\sigma} - \mathcal{F}_{n\sigma}$ regions, respectively, have effectively the same form of the integral over $q_\perp$, given by Eq. (29), while the corresponding line integrals are along the curves $\mathcal{C}^>_{n\sigma}$ and $\mathcal{C}^<_{n\sigma}$. As the two curves together constitute the whole FS sheet $\mathcal{C}_{n\sigma}$ of band $n\sigma$, the sum of the second and third terms in Eq. (24) is given by the line integral along $\mathcal{C}_{n\sigma}$. The form of the integrated expression (29) can be further simplified by noting that the change of the Fermi energy $\delta\epsilon_{\mathrm{F}}$ is of the second order in the SOC, regardless of the presence or absence of the inversion symmetry, as shown within the finite-temperature approach in Ref. [6] and for $T = 0$ in Appendix A in this work. The term $(\delta\epsilon_{\mathrm{F}})^2 \sim O(H_{\mathrm{so}}^4)$ can be then neglected in Eq. (29) while $(\delta\epsilon_{n\sigma})^2$ can be replaced with its leading contribution $(\epsilon^{(1)}_{n\sigma})^2$ so that the sum of the second and third terms in Eq. (24) results in the following second-order term of the band energy:

$$\begin{aligned} E_{\mathrm{b}}^{(2')} &= -\frac{1}{2}\frac{1}{\Omega_{2\mathrm{D}}}\sum_{n\sigma}\int_{\mathcal{C}_{n\sigma}} ds\,\frac{\left[\epsilon^{(1)}_{n\sigma}(\mathbf{k}_s)\right]^2}{|\nabla_{\mathbf{k}}\epsilon_{n\sigma}(\mathbf{k}_s)|} \\ &= -\frac{1}{2}\frac{1}{\Omega_{2\mathrm{D}}}\sum_{n\sigma}\int_{\mathcal{C}_{n\sigma}} ds\,\frac{|\langle n\mathbf{k}_s\sigma|H_{\mathrm{SO}}|n\mathbf{k}_s\sigma\rangle|^2}{|\nabla_{\mathbf{k}}\epsilon_{n\sigma}(\mathbf{k}_s)|} \end{aligned} \tag{33}$$

given by the sum of line integrals along the different FS sheets $\mathcal{C}_{n\sigma}$.

Thus, we obtain the PT expansion of the band energy at $T = 0$:

$$E_{\mathrm{b}} = E_{\mathrm{b}}^{(0)} + E_{\mathrm{b}}^{(1)} + E_{\mathrm{b}}^{(2)} + E_{\mathrm{b}}^{(2')} \tag{34}$$

which includes, apart from the usual interband term $E_{\mathrm{b}}^{(2)}$ given by Eq. (21), another second-order contribution $E_{\mathrm{b}}^{(2')}$

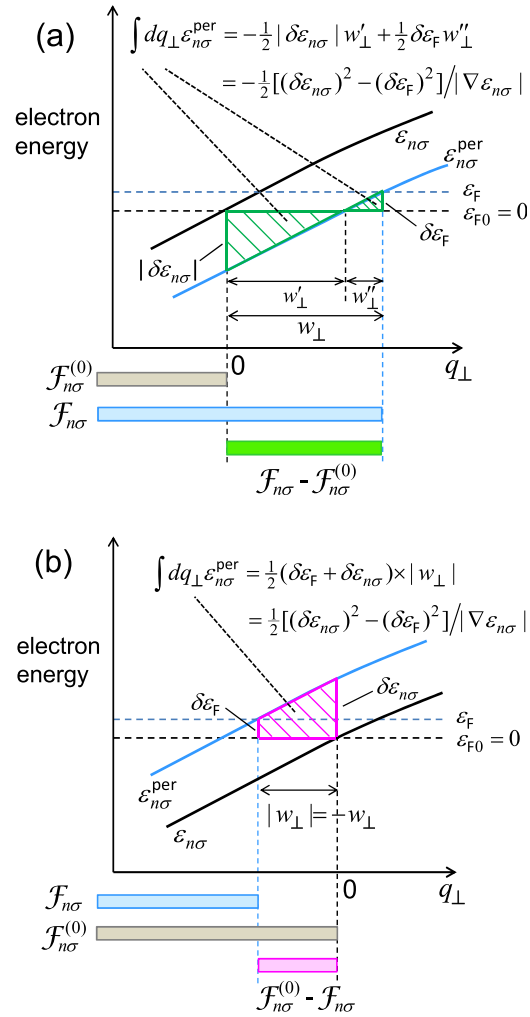

FIG. 2. Geometrical interpretation of the contributions to the system band energy E_{b} from the perturbed energy band $n\sigma$ in the two stripe-shaped subsets of the BZ, (a) $\mathcal{F}_{n\sigma} - \mathcal{F}^{(0)}_{n\sigma}$ and (b) $\mathcal{F}^{(0)}_{n\sigma} - \mathcal{F}_{n\sigma}$ [see Fig. 1 and Eq. (24), its second and third terms]. The visualized contributions, given by Eqs. (29) and (32), are the integrals of $\epsilon^{\mathrm{per}}_{n\sigma} = \epsilon_{n\sigma} + \delta\epsilon_{n\sigma}$ over the intervals (a) $0 < q_\perp < w_\perp$ and (b) $-|w_\perp| < q_\perp < 0$ of the axes perpendicular to the FS sheet $C_{n\sigma}$ at the points (a) $\mathbf{k}_s \in C^>_{n\sigma}$ for $\delta\epsilon_{n\sigma} < 0 < \delta\epsilon_{\mathrm{F}}$ and (b) $\mathbf{k}_s \in C^<_{n\sigma}$ for $0 < \delta\epsilon_{\mathrm{F}} < \delta\epsilon_{n\sigma}$, respectively. The $q_\perp$ axis crosses the FS sheet at $q_\perp = 0$. The stripe width is equal to (a) $w_\perp$ [Eq. (27)] or (b) its negative $-w_\perp$, and, in case (a), is the sum of $w'_\perp = |\delta\epsilon_{n\sigma}|/|\nabla_{\mathbf{k}}\epsilon_{n\sigma}|$ and $w''_\perp = \delta\epsilon_{\mathrm{F}}/|\nabla_{\mathbf{k}}\epsilon_{n\sigma}|$ at $\mathbf{k} = \mathbf{k}_s$. The zero-energy level is chosen at the Fermi energy $\epsilon_{\mathrm{F}0} = 0$.

which comes from the change of state occupations near the Fermi level due the SOC perturbation. This additional term, which comprises $(\epsilon^{(1)}_{n\sigma})^2$, is finite only for systems without the inversion symmetry, where the first-order corrections $\epsilon^{(1)}_{n\sigma}$ do not necessarily vanish, and has exactly the same form as the $T \to 0$ limit of the intraband term of $F^{(2)} = \Omega^{(2)}$ [Eq. (19)]. Thus, the above-raised concern about the apparent discrepancy between the $T \to 0$ limit of $F^{(2)}$ and the second-order term of E_{b} at $T = 0$ is resolved. The same result for the band energy at $T = 0$ is obtained from the power-series expansion of the occupation factors $\theta(\epsilon_{\mathrm{F}} - \epsilon^{\mathrm{per}}_{n\sigma}) = \theta[\epsilon_{\mathrm{F}0} -$

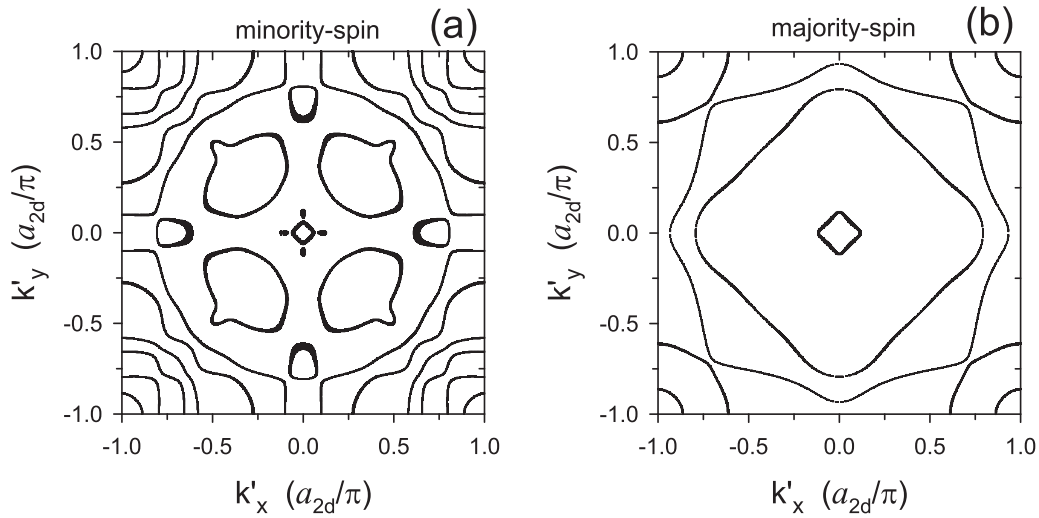

FIG. 3. FS sheets for (a) minority-spin and (b) majority-spin electrons in (001) fcc Co(2 ML)/Pd(2 ML) in the absence of the SOC found using a realistic tight-binding model [6,8,9]. The plotted sheets are determined as the set of **k** points where there are electron states with energies closer than 0.003 eV from the Fermi energy. The k'_x and k'_y axes are along the $(1\bar{1}0)$ and (110) axes, respectively.

$\epsilon_{n\sigma} + (\delta\epsilon_F - \delta\epsilon_{n\sigma})]$ in the perturbed system (θ is the unit step function); this alternative derivation is given in Appendix B. However, such a direct approach does not give a good insight into the origin of the intraband term of the MCA energy while the discussion presented in this section clearly reveals the mechanism of how this term arises.

This discussion can also be illustrated with an exemplary plots of the actual FS sheets for a thin Co/Pd bilayer with and without the SOC; see Figs. 3 and 4. It is found that the pattern of the FS sheets behaves according to the presented above description in most of the BZ so that the FS sheet curves slightly change their shapes and positions upon the introduction of the SOC and the regions where the occupation of states from a specific energy band changes are narrow stripes of a variable width. The shape of the FS sheets is modified by the SOC in a more significant way close to the center of the BZ where the bands are flatter which results in smaller gradients $\nabla_{\mathbf{k}}\epsilon_{n\sigma}$ and thus larger stripe widths $|w_\perp|$, according Eq. (27). Note that the curves of the unperturbed FS sheets shown in Fig. 3 do not cross each other or stick together at some **k** points, even on the high-symmetry lines and at the high-symmetry points. This means that there are no degenerate states of the same spin at the Fermi level in the investigated Co(2 ML)/Pd (2 ML) bilayer which supports the

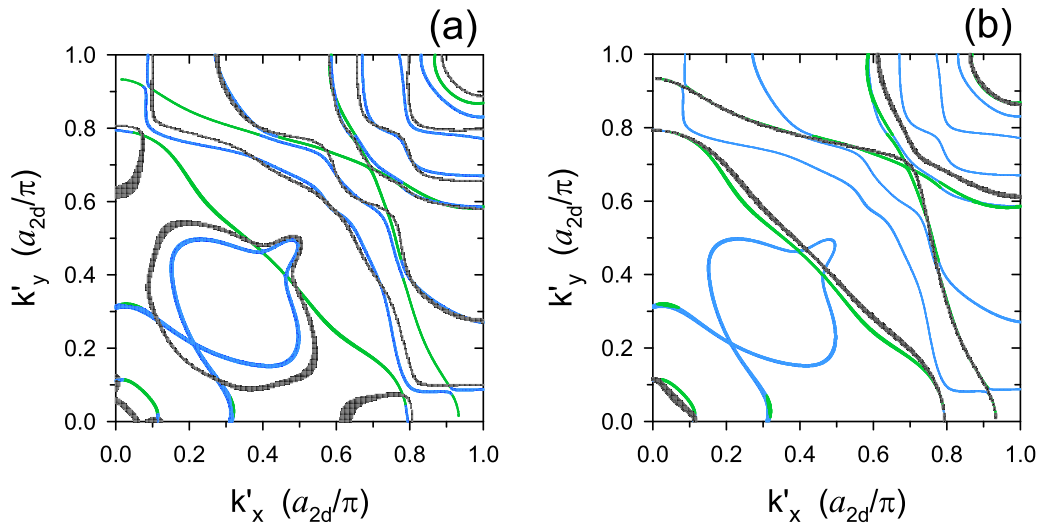

FIG. 4. (a), (b) FS sheets obtained with the SOC included (blue and green lines) for (001) fcc Co(2 ML)/Pd(2 ML) bilayer with the magnetization along the (100) axis. The sheets are coloured according to the dominating spin component in the respective electron states, with the spin-projected occupation number larger than 0.5 for minority spin (blue lines) or majority spin (green lines). For comparison, the FS sheets found without the SOC (dark grey lines) for (a) minority-spin and (b) majority-spin electrons are also drawn. The sheets in one quarter of the BZ are shown.

theoretical arguments for the absence of such states in layered systems of a cubic structure and the (001) surface, presented in the last paragraph of Sec. II A.

The calculation of the MCA intraband terms using the line integrals along the FS sheets curves is computationally cumbersome, or even hardly doable. Indeed, the numerical implementation of such a method is not straightforward, in particular, because one needs to determine a large number of the FS sheets which is considerable even for very thin systems (Fig. 3) and grows linearly with increasing the film thickness. Thus, the finite-temperature formulation based on Eq. (11) is much more convenient in the actual calculations of the MCA energy within the PT approach. The integration over $\mathbf{k}$ is then performed over the whole BZ, for both intraband and interband terms of this energy.

Note, however, it is still possible to calculate the MCA energy at $T = 0$ without determining the troublesome line integrals along the FS sheets, by applying the triangle method [55,56] which is the two-dimensional counterpart of the tetrahedron method [57,58] used for three-dimensional crystals. The two-dimensional BZ is then divided into a triangular grid and the integrals over $\mathbf{k}$, like those in Eqs. (17) and (20), are calculated analytically for each triangle after the energies $\epsilon_{n\sigma}(\mathbf{k})$ and the accompanying factors, like $|\epsilon^{(1)}_{n\sigma}(\mathbf{k})|^2$, are approximated by the linear interpolation inside the triangle based on values of these quantities at the triangle corners. In particular, the intraband term $E_{\rm b}^{(2')}$ is calculated by a straightforward modification of the analytical expression for the orbital-projected DOS given in Ref. [56]. In this way, the intraband term of the MCA energy at $T = 0$ can be represented by a sum over the grid nodes. The interband term $E_{\rm b}^{(2)}$ of the band energy at $T = 0$, defined in Eq. (20), can also be calculated with the triangle method using the analytical expression for the integral of $\theta[\epsilon_{\rm F0} - \epsilon_{n\sigma}(\mathbf{k})]\theta[\epsilon_{n'\sigma'}(\mathbf{k}) - \epsilon_{\rm F0}][\epsilon_{n\sigma}(\mathbf{k}) - \epsilon_{n'\sigma'}(\mathbf{k})]^{-1}$ over a triangle which was reported in Ref. [1] and successfully applied for ferromagnetic films of Fe, Co, and Ni therein. However, the use of the triangle method in calculation of $E_{\rm b}^{(2)}$ requires extra care in numerical implementation, especially when the energies at two or three corners are equal or close to one another. In addition, a much larger number of $\mathbf{k}$ points is needed for convergence of the MCA energy calculated with this method at $T = 0$ compared to the finite-temperature approach based on Eq. (11) at $T = 300$ K [9]. Thus, the latter approach is preferable in the numerical calculations of the MCA energy with the PT. The triangle method can also be used to obtain convergent values of the MCA energy with the FT at $T = 0$. In doing so, the band energy, expressed as $E_{\rm b} = \int_{-\infty}^{\epsilon_{\rm F}} \epsilon n(\epsilon) d\epsilon$, is found by integrating the analytical formula obtained for the DOS $n(\epsilon)$ [55].

C. Representation of MCA energy with SOC energy including intraband terms

The MCA energy can also be represented as half the difference of the SOC energies for the two magnetization directions

$$E_{\rm MCA} = \tfrac{1}{2}\Delta E_{\rm SOC} = \tfrac{1}{2}[E_{\rm SO}(\hat{\mathbf{M}}_\perp) - E_{\rm SO}(\hat{\mathbf{M}}_\parallel)], \tag{35}$$

where the SOC energy

$$E_{\rm SO}(\hat{\mathbf{M}}) = \frac{1}{\Omega_{\rm 2D}} \int d\mathbf{k} \sum_m f(\epsilon_m(\mathbf{k}))\, \langle m\mathbf{k}|H_{\rm SO}|m\mathbf{k}\rangle \tag{36}$$

is calculated with the occupied states $|m\mathbf{k}\rangle$ found by direct diagonalization of the perturbed Hamiltonian $H + H_{\rm SO}$. This method largely resembles the FT approach of Eq. (3) where the MCA energy is expressed by the difference of the free energies $F(\hat{\mathbf{M}}_\perp) - F(\hat{\mathbf{M}}_\parallel)$ which reduces to $E_{\rm b}(\hat{\mathbf{M}}_\perp) - E_{\rm b}(\hat{\mathbf{M}}_\parallel)$ at $T = 0$. However, the above representation of the MCA energy with the SOC energy is not fully equivalent to the FT approach and, in fact, the formula (36) is derived within the PT framework.

The derivation given in Ref. [41] is based on the assumption that the N-electron ground state of the system perturbed by the SOC can be obtained within the PT as the perturbed N-electron ground state of the unperturbed system. In fact, since the MCA energy is defined with the system's band energies, the above assumption should be referred to the N-electron ground state of the noninteracting Kohn-Sham system (with and without the SOC) which is used to describe the real interacting system within the DFT. The energy of this state is the band energy $E_{\rm b}$ given by Eq. (2) and its N-electron wave function is the Slater determinant built of the wave functions of all occupied electron states. Thus, the electron states which are occupied in the ground state of the unperturbed system are assumed to remain occupied after the perturbation is introduced. As result, the PT correction to the energy $E_{\rm b}^{(0)}$ of this system is given by the second-order interband term $E_{\rm b}^{(2)}$ built of the second-order corrections $\epsilon^{(2)}_{n\sigma}$ to the energies of these electron states, Eq. (21). However, as already shown and discussed in detail above, such an assumption about the occupations of electron states is not usually true for extended metallic systems, like the presently investigated layered structures, and, as result, the second-order intraband term $E_{\rm b}^{(2)}$ does not represent the whole second-order contribution of the SOC perturbation to the band energy $E_{\rm b}$. Thus, for systems without the inversion symmetry, where the finite intraband contribution $E_{\rm b}^{(2')}$ is present in addition to $E_{\rm b}^{(2)}$, the proof of the relation (35) needs suitable amendments. This can be readily done within the present finite-temperature formulation as follows.

The SOC energy given by Eq. (36) can be expressed, up to the second order in the SOC, with the first-order PT expansions for the perturbed eigenstates

$$|m\mathbf{k}\rangle = |n\mathbf{k}\sigma\rangle^{\rm per} = |n\mathbf{k}\sigma\rangle + \sum_{n'\sigma'\neq n\sigma} \frac{\langle n'\mathbf{k}\sigma'|H_{\rm SO}|n\mathbf{k}\sigma\rangle}{\epsilon_{n\sigma}(\mathbf{k}) - \epsilon_{n'\sigma'}(\mathbf{k})}\, |n'\mathbf{k}\sigma'\rangle, \tag{37}$$

and their energies $\epsilon_m = \epsilon^{\rm per}_{n\sigma} = \epsilon_{n\sigma} + \epsilon^{(1)}_{n\sigma}$, alongside the following expansion of the occupation factors:

$$\begin{aligned} f(\epsilon_m) &= f(\epsilon^{\rm per}_{n\sigma}) = f(\epsilon_{n\sigma} + \epsilon^{(1)}_{n\sigma}) = f_0(\epsilon_{n\sigma} + \epsilon^{(1)}_{n\sigma} - \delta\epsilon_{\rm F}) \\ &= f_0(\epsilon_{n\sigma}) + f_0'(\epsilon_{n\sigma})(\epsilon^{(1)}_{n\sigma} - \delta\epsilon_{\rm F}). \end{aligned} \tag{38}$$

The first-order term of $E_{\rm so}$ vanishes,

$$\frac{1}{\Omega_{\rm 2D}} \int d\mathbf{k} \sum_{n\sigma} f_0(\epsilon_{n\sigma}(\mathbf{k}))\langle n\mathbf{k}\sigma|H_{\rm SO}|n\mathbf{k}\sigma\rangle = 0, \tag{39}$$

with $\langle n\mathbf{k}\sigma|H_{\rm SO}|n\mathbf{k}\sigma\rangle = 0$ for systems with the inversion symmetry or due to the cancellation of $\mathbf{k}$ and $-\mathbf{k}$ contributions if this symmetry is absent, as it is explained above (in fact, this term is equal to $F^{(1)} = \Omega^{(1)} = 0$). The shift $\delta\epsilon_{\rm F} = \epsilon_{\rm F} - \epsilon_{\rm F0}$ of the Fermi energy present in Eq. (38) is of the second order in the SOC [6] so that it contributes to $E_{\rm SO}$ in Eq. (36) only in the third and higher orders. Thus, the remaining terms in the expansion of the SOC energy are of the second order and give the following PT representation of this energy with unperturbed states and their energies:

$$E_{\rm SO} = \frac{1}{\Omega_{\rm 2D}} \int d\mathbf{k} \sum_{n\sigma} f\left(\epsilon^{\rm per}_{n\sigma}(\mathbf{k})\right) {}^{\rm per}\langle n\mathbf{k}\sigma|H_{\rm SO}|n\mathbf{k}\sigma\rangle^{\rm per}$$
$$= \frac{1}{\Omega_{\rm 2D}} \int d\mathbf{k} \sum_{n\sigma} \sum_{n'\sigma'} \frac{f_0(\epsilon_{n\sigma}(\mathbf{k})) - f_0(\epsilon_{n'\sigma'}(\mathbf{k}))}{\epsilon_{n\sigma}(\mathbf{k}) - \epsilon_{n'\sigma'}(\mathbf{k})}$$
$$\times |\langle n'\mathbf{k}\sigma'|H_{\rm SO}|n\mathbf{k}\sigma\rangle|^2 = 2F^{(2)}. \quad (40)$$

The intraband contributions ($n\sigma = n'\sigma'$), equal to $f_0'(\epsilon_{n\sigma})|\langle n\mathbf{k}\sigma|H_{\rm SO}|n\mathbf{k}\sigma\rangle|^2$, come from the term $f_0'(\epsilon_{n\sigma})\epsilon^{(1)}_{n\sigma}$ in the expansion (38), multiplied by $\langle n\mathbf{k}\sigma|H_{\rm SO}|n\mathbf{k}\sigma\rangle = \epsilon^{(1)}_{n\sigma}$, so they arise in a similar way as in the PT expansion of the free energy $F = F_0 + F^{(2)}$ where the same intraband terms $\frac{1}{2}f_0'(\epsilon_{n\sigma})(\epsilon^{(1)}_{n\sigma})^2$ result from the expansion of the function $g(\epsilon^{\rm per}_{n\sigma}) = g(\epsilon_{n\sigma} + \epsilon^{(1)}_{n\sigma} + \epsilon^{(2)}_{n\sigma})$ up to the second order (see the Appendix in Ref. [6]).

Thus, according to Eqs. (11), (12) and (35), (40), half of the SOC energy difference $\Delta E_{\rm SO}/2$ reproduces the leading (second-order) term in the PT expansion of the MCA energy, including the finite intraband terms present in the absence of the inversion symmetry. However, the higher-order terms of the two quantities can still differ so the alternative representation of the MCA energy with Eq. (35) derived using the PT is not expected to exactly reproduce the reference values of this energy obtained with the FT.

III. RESULTS

A. Intraband and interband terms of MCA energy for Co film and Co/X layered systems with X = Cu and Pd

The theoretical discussion on the intraband terms of the MCA energy presented in the previous section is now supplemented with the numerical results for a few exemplary magnetic layered systems. The selected systems have the fcc structure and include a ferromagnetic Co layer with the thickness up to 22 monolayers (ML); some of the systems possess the inversion symmetry while others do not. The calculations of the MCA energy are mainly done within the finite-temperature formulation (Sec. II A) at $T = 300$ K using a realistic tight-binding (TB) model of electronic structure. The applied TB model includes the shifts of onsite orbital energies to make each atomic layer electrically neutral and is described in detail in Refs. [3,8,9]. The assumed values of the SOC constants for Co, Cu, and Pd are $\xi_{\rm Co} = 0.085$ eV, $\xi_{\rm Cu} = 0.1$ eV and $\xi_{\rm Pd} = 0.23$ eV, respectively [59]. The MCA energies are determined with the accuracy of 0.01 meV/(surface atom), both in the FT and PT approaches, which, at $T = 300$ K, is reached by summing contributions from the number $N_{\rm 2D} = 3600$–6400 of $\mathbf{k}$ points from the whole BZ. The convergence of integration over the BZ and selected results

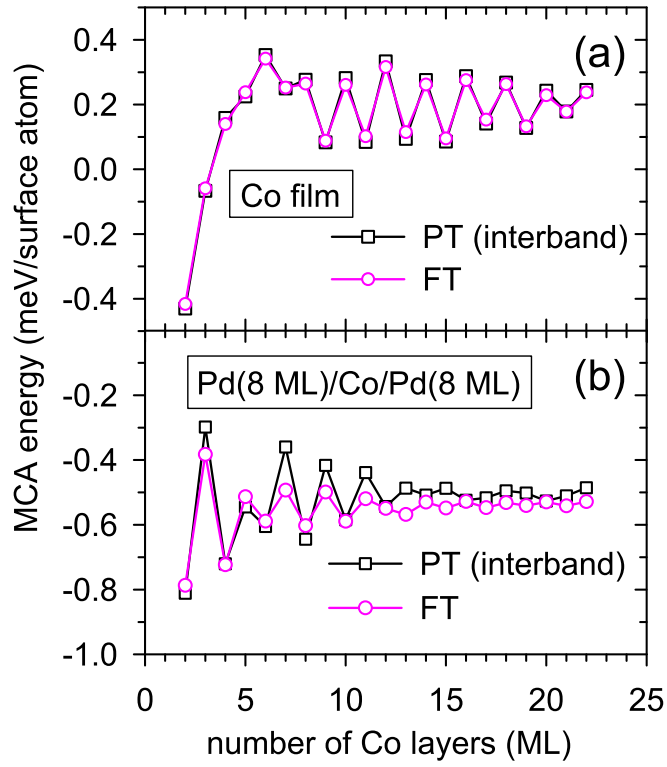

FIG. 5. MCA energy obtained with the PT formula (14) including only interband contributions (black squares) for the (001) fcc (a) Co film and (b) Pd(8)/Co/Pd(8 ML) trilayer compared with the MCA energy found for these systems with the FT (pink circles).

for other temperatures, including $T = 0$, are discussed in Sec. III B. Note that the same scheme of thermal smearing is applied in the MCA calculations with the FT and PT since the expression for $F^{(2)}$, Eq. (11), is derived by the perturbation expansion of the free energy F, which is used to define the MCA energy with the FT in Eq. (3).

It is confirmed that for a free-standing Co film and a symmetric Pd/Co/Pd trilayer, which both have the inversion symmetry, the intraband term of the MCA energy

$$E_{\rm MCA,intra} = F^{(2)}_{\rm intra}(\hat{\mathbf{M}}_\perp) - F^{(2)}_{\rm intra}(\hat{\mathbf{M}}_\parallel) \quad (41)$$

vanishes and the standard PT formula [1,28,29] including only the interband term

$$E_{\rm MCA,inter} = F^{(2)}_{\rm inter}(\hat{\mathbf{M}}_\perp) - F^{(2)}_{\rm inter}(\hat{\mathbf{M}}_\parallel) \quad (42)$$

very well reproduces the exact $E_{\rm MCA}$ calculated with the FT (see Fig. 5). The situation is different for systems that lack the inversion symmetry. A large discrepancy between the results of the two methods is found for the Co/Pd(8 ML) bilayer (Fig. 6) as the MCA energies given by such an incomplete PT formula are about 1 meV/(surface atom) lower than the actual MCA energies obtained with the FT. However, the inclusion of the intraband term alongside the interband one comes as an immediate remedy to this problem since the sum of the two terms, leading to the full PT formula represented by Eqs. (11) and (12), gives the total MCA energy in very good agreement with the FT result. Even better agreement is reached for the Co/Cu(8 ML) bilayer (Fig. 7). It is also shown that the representation of the MCA energy as the half SOC energy

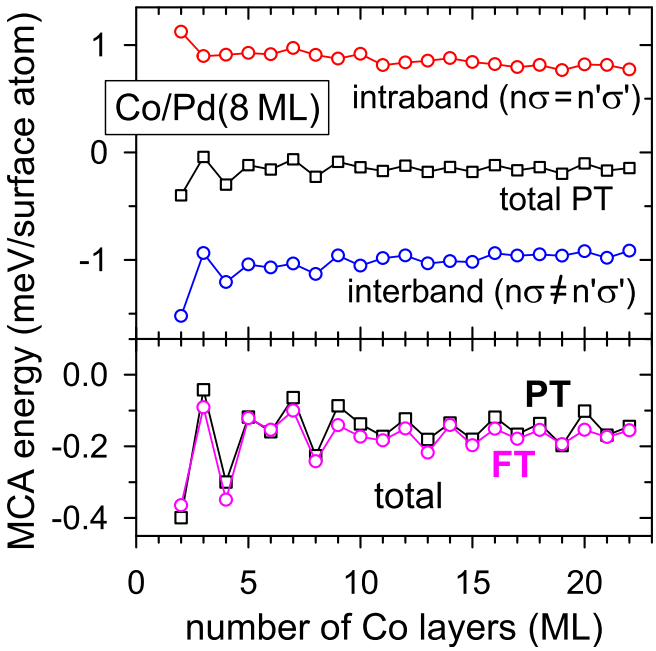

FIG. 6. Intraband (red circles) and interband (blue circles) terms of the total MCA energy (black squares) obtained within the PT [Eqs. (15), (14), and (13), respectively] for the (001) fcc Co/Pd (8 ML) bilayer compared with the MCA energy found with the FT (pink circles).

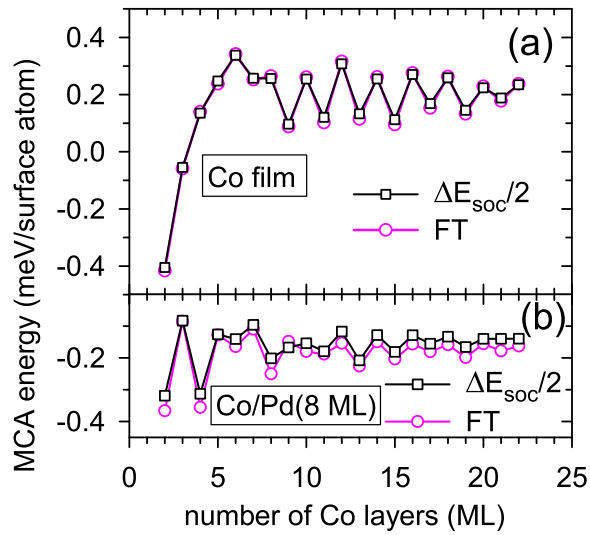

FIG. 8. MCA energy E_{MCA} of the (001) fcc (a) Co film and (b) Co/Pd(8 ML) bilayer calculated as $\frac{1}{2}\Delta E_{\mathrm{SOC}}$ (black squares) with Eq. (35) and compared to the exact E_{MCA} (pink circles) obtained with the FT using Eq. (3).

difference $\frac{1}{2}\Delta E_{\mathrm{SOC}}$, Eq. (35), is almost exact for the Co film and only slightly less accurate for the Co/Pd bilayer (Fig. 8), thus providing a numerical confirmation that this representation is valid for systems with and without the inversion symmetry, respectively, as argued theoretically in Sec. II C.

For both considered bilayers, the intraband term of the MCA energy is of similar magnitude as its interband term and the two terms largely cancel out when they are added to give the total value of this energy. The accuracy with which the MCA energy found with the FT is reproduced by the second-order PT formula is largely related to the strength of the SOC perturbation. The agreement is almost perfect for the Co film and the Co/Cu bilayer, and still very good for the Co/Pd bilayer, while, as shown in Ref. [6], it is much worse for the Co/Pt bilayer, comprising the Pt layer with a very strong SOC. For the latter system, the PT formula predicts that the oscillations of the MCA energy versus the Co thickness have much larger amplitude than in the FT approach while the mean value of this energy is roughly reproduced by the PT. This is an interesting finding whose origin remains to be explained.

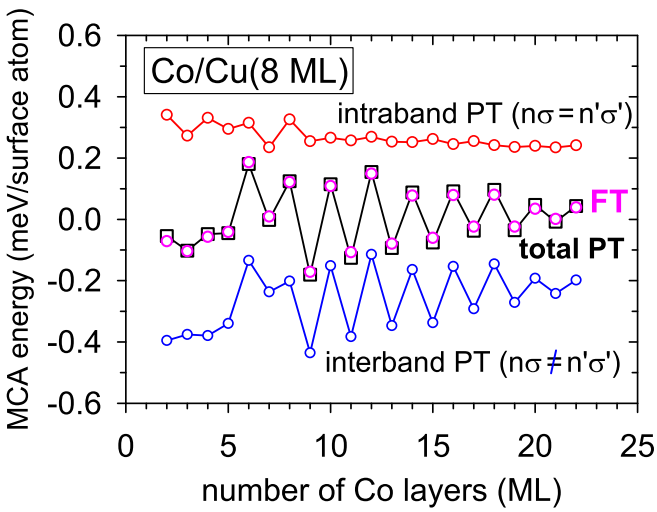

FIG. 7. Intraband (red circles) and interband (blue circles) contributions to the total MCA energy (black squares) obtained with the PT for the (001) fcc Co/Cu(8 ML) bilayer compared with the MCA energy found with the FT (pink circles).

The very existence of the large second-order intraband terms in the MCA energy for the Co/X bilayers is not conditioned by the presence of the SOC in the nonmagnetic layer of the metal X but results from the modification of the electronic structure within the Co layer due to the presence of this overlayer. Such a modification changes the effect of the SOC in Co on the bilayer energy, or its free energy (in particular, by leading to the finite diagonal matrix elements of H_{SO}), and, consequently, affects the MCA energy. To verify this explanation, the MCA energy is also determined for a Co/Pd bilayer system with no SOC in the Pd layer [Fig. 9(a)]. It is found that, for this system too, the intraband and interband terms are both sizable and of very similar magnitude, though smaller (around three times) than for the Co/Pd bilayer with the normal SOC in Pd.

A similar test for the Co/Cu bilayer [Fig. 9(b)] shows that the full quenching of the SOC in Cu has little effect on the MCA energy, both its intraband and interband terms. This happens because the matrix elements $\langle n'\mathbf{k}\sigma'|H_{\mathrm{so}}|n\mathbf{k}\sigma\rangle$ that significantly contribute in the PT formula (11) are weakly affected by the strength of the SOC in Cu since the electron states with energies around the Fermi level ϵ_{F0} are localized mostly within the Co layer, with very small amplitudes inside the Cu layer. Such a localization is confirmed by a very

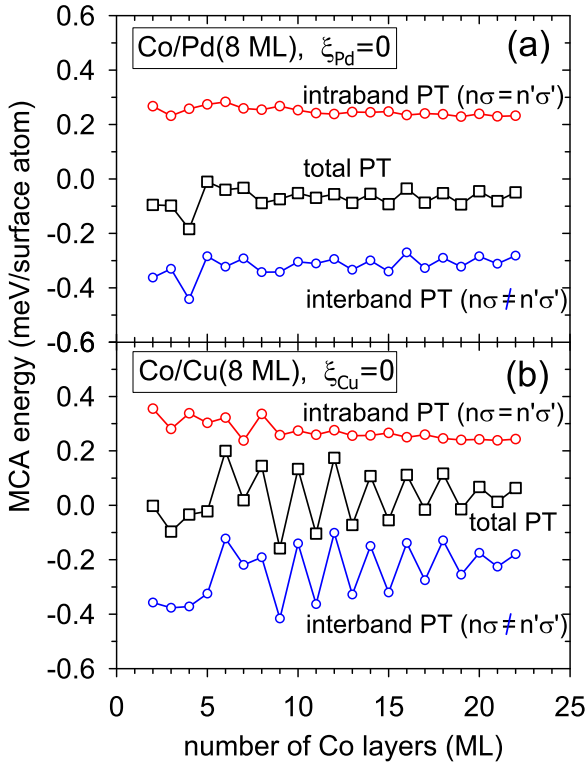

FIG. 9. Intraband (red circles) and interband (blue circles) contributions to the total MCA energy (black squares) obtained with the PT [Eqs. (15), (14), and (13), respectively] for the (001) fcc (a) Co/Pd(8 ML) and (b) Co/Cu(8 ML) bilayers with no SOC in the Pd and Cu layers ($\xi_{\mathrm{Cu}} = 0$ and $\xi_{\mathrm{Pd}} = 0$).

low layer-projected DOS in all Cu atomic layers for energies higher than around $\epsilon_{\mathrm{F0}} - 1.5$ eV (see, e.g., Ref. [60]), i.e., above the upper edge of the d band in bulk Cu. The localization of electrons with such energies inside the Co layer means that, for these electrons, the Co/Cu interface effectively works as a potential wall of a finite height so that a quantum well is formed in the Co layer. This results in large 2-ML-period oscillations of the MCA energy versus the Co thickness for the Co/Cu bilayer, in a similar way as for the Co film where a similar quantum well is defined by the two Co/vacuum interfaces [3].

The situation is different for Co/Pd bilayers where electron states with energies close to ϵ_{F0} can span over the whole bilayer since the d band in Pd crosses the Fermi level. As a result, modifying the SOC strength in Pd has a significant impact on the matrix elements of H_{SO} and, consequently, the magnitude of the MCA energy and its both terms (intraband and interband), though, still the intraband term does not vanish for $\xi_{\mathrm{Pd}} = 0$, as noted above. It is also found that the presence of the d states in Pd which the d states in Co with energies around ϵ_{F0} can hybridize with has also a strong effect on the 2-ML-period oscillations of the MCA energy with increasing the Co thickness. In particular, the oscillation amplitude is largely reduced in comparison with the Co/Cu bilayer and the Co film. Nevertheless, since the oscillatory patterns of the MCA energies have the clear 2-ML dominating period for all investigated systems (Figs. 5–7) the MCA energy oscillations vs the Co thickness are expected to come from pairs of quantum-well d states which are degenerate at the $\overline{\Gamma}$ point and originate from the fcc Co bulk band of the Δ_5 symmetry, just as it has been shown for a freestanding Co film [3].

The obtained intraband term of the MCA energy $E_{\mathrm{MCA,intra}}$ [Eq. (41)] is positive for both Co/Cu and Co/Pd bilayers. In fact, this is true for all the layered systems with a cubic symmetry, the (001) surface and a collinear magnetization that do not have the inversion symmetry since for such systems the second-order intraband term $F^{(2)}_{\mathrm{intra}}$ of the free energy, Eq. (15), is finite and negative for the in-plane magnetization while vanishing for the out-of-plane magnetization (note that $F^{(2)}_{\mathrm{intra}}$ is nonpositive for any layered system and magnetization direction). Indeed, if the magnetization is along the z axis ($\hat{\mathbf{M}} = \hat{\mathbf{M}}_{\perp}$) the matrix element $\langle n\mathbf{k}\sigma|H_{\mathrm{SO}}|n\mathbf{k}\sigma\rangle$ is equal to $\pm\frac{1}{2}\langle n\mathbf{k}\sigma|\mathcal{O}_z|n\mathbf{k}\sigma\rangle$ where $\mathcal{O}_z(\mathbf{r}) = \sum_{lj}\xi_l L_z(\mathbf{r} - \mathbf{R}_{lj})$ [see Eq. (1)]. For layered systems with the in-plane inversion symmetry, like the (001) fcc Co/X bilayers, the operator $\mathcal{O}_z(\mathbf{r})$ remains unchanged under the respective transformation $\boldsymbol{\rho} = (x, y) \to (-x, -y) = -\boldsymbol{\rho}$ and becomes equal to $-\mathcal{O}_z(\mathbf{r})$ if this transformation is followed by the complex conjugation. Since the unperturbed Hamiltonian $H(\mathbf{r})$ is invariant under each of the two transformations, the transformed states $|n\mathbf{k}\sigma\rangle$ are also eigenstates of H with the same energy $\epsilon_{n\sigma}(\mathbf{k})$. Thus, for a nondegenerate state $|n\mathbf{k}\sigma\rangle$ at a general $\mathbf{k}$ point, the combined action of these two symmetry operations on the wave function $\psi^{\sigma}_{n\mathbf{k}}(\mathbf{r}) = e^{i\mathbf{k}\boldsymbol{\rho}}u^{\sigma}_{n\mathbf{k}}(\mathbf{r})$, which leaves the Bloch prefactor $e^{i\mathbf{k}\boldsymbol{\rho}}$ unchanged, gives the same wave function up to a constant phase factor $[\psi^{\sigma}_{n\mathbf{k}}(-x, -y, z)]^* = e^{i\alpha}\psi^{\sigma}_{n\mathbf{k}}(x, y, z)$, where $\alpha = \alpha^{\sigma}_{n\mathbf{k}}$. In this way, by applying such a composed symmetry operation, it can be shown that the real matrix element $\langle n\mathbf{k}\sigma|\mathcal{O}_z|n\mathbf{k}\sigma\rangle = \int d\mathbf{r}[\psi^{\sigma}_{n\mathbf{k}}(\mathbf{r})]^*\mathcal{O}_z(\mathbf{r})\psi^{\sigma}_{n\mathbf{k}}(\mathbf{r})$ is equal to $-\langle n\mathbf{k}\sigma|\mathcal{O}_z|n\mathbf{k}\sigma\rangle$ so it must vanish and, as a result, we obtain $F^{(2)}_{\mathrm{intra}} = 0$ for $\hat{\mathbf{M}} = \hat{\mathbf{M}}_{\perp}$. This conclusion does not hold for the intraband term $F^{(2)}_{\mathrm{intra}}$ with magnetization in the x direction ($\hat{\mathbf{M}} = \hat{\mathbf{M}}_{\parallel}$) since the respective operator $\mathcal{O}_x(\mathbf{r}) = \sum_{lj}\xi_l L_x(\mathbf{r} - \mathbf{R}_{lj})$ which defines the SOC for this direction of the net spin remains unchanged after the two symmetry operations are applied: $[\mathcal{O}_x(-x, -y, z)]^* = \mathcal{O}_x(-x, -y, z)$. The above reasoning is based on similar arguments as those used to show that the diagonal matrix elements of H_{SO} and the system's orbital angular momentum (its all components, in x, y, and z directions) vanish for systems with the full (three-dimensional) inversion symmetry for any magnetization direction (see Appendix A in Ref. [9] for more details).

B. Dependence of MCA energy on thermal smearing and convergence of the Brillouin zone integration

Although the finite temperature is introduced to smear the electron energy levels and thus improve the convergence of the calculated MCA energies, such a smearing also leads to some physical effects. In particular, it is found that the amplitude of the MCA energy oscillations is reduced with increasing the temperature [9] which is confirmed experimentally for Fe and Co films [12,14]. To demonstrate the effect of temperature, the MCA energy of the Co/Pd(8 ML) bilayer is also calculated for finite temperatures lower than 300 K, down to 50 K, with both the FT and PT using Eqs. (3) and (12), respectively. In addition, a separate calculation of the MCA energy with the two methods is done for the ground

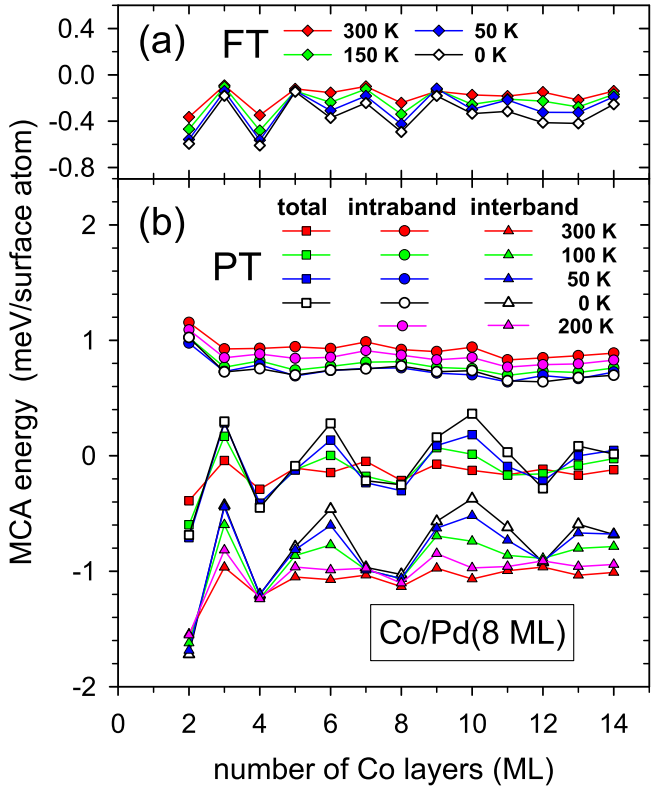

FIG. 10. MCA energy (diamonds, squares) of the (001) fcc Co/Pd(8 ML) bilayer calculated with the (a) FT and (b) PT for finite temperatures and $T = 0$. (b) The intraband (circles) and interband (triangles) terms of the MCA energy. The results are obtained with $N_k = 70$ that defines the number $N_{2D} = (2N_k + 1) \times (2N_k + 1)$ of **k** points used for the integration over the BZ.

state ($T = 0$), using the triangle method for integration over the BZ in Eqs. (2), (17), and (20), as described in the last part of Sec. II B.

It is found [Fig. 10(b)] that the intraband term $E_{\mathrm{MCA,intra}}$ of the MCA energy is very similar for all temperatures, being only slightly shifted at finite temperatures compared to $T = 0$. The shift is almost independent of the Co thickness, it is around 0.2 meV/(surface atom) at $T = 300$ K and decreases as the temperature gets smaller so that the term $E_{\mathrm{MCA,intra}}$ at $T = 50$ K is almost equal to its value in the ground state ($T = 0$). The effect of smearing the electron energies by finite temperature is different for the interband term $E_{\mathrm{MCA,inter}}$. While this effect is almost negligible for some Co thicknesses the value of $E_{\mathrm{MCA,inter}}$ significantly changes (grows) with decreasing the temperature for other Co thicknesses and the change is the stronger the lower temperature is. This leads to the oscillations of the total MCA energy which, evidently, come mostly from its interband term, especially at low temperatures. The effect can be attributed to quantum-well states which cross the Fermi energy in a regular manner as the thickness of the Co layer grows and couple to other states which also lie close to ϵ_F. In fact, such a mechanism of the MCA oscillations has been previously [3] established for free-standing Co films where pairs of quantum-well d states with closely lying energies, degenerate at the $\overline{\Gamma}$ point, are present and cross ϵ_F.

Oscillations with the amplitude which grows with decreasing the temperature are also present in the MCA energy obtained with the FT [see Fig. 10(a)]. However, while the values of E_{MCA} obtained for the Co/Pd(8 ML) bilayer with the FT and PT nearly coincide at $T = 300$ K, their oscillatory patterns become increasingly different as the temperature gets lower. The oscillation amplitude of $E_{\mathrm{MCA}}(N_{\mathrm{Co}})$ is significantly smaller for the MCA energies found with the FT than for those obtained with the PT. This could be explained by assuming that, at lower temperatures, the validity of the PT approach to the MCA is compromised at lower strengths of the SOC perturbation so that the significant discrepancy between the FT and PT results, previously found for the MCA energies of the Co/Pt bilayers at $T = 300$ K [6], also occurs for the Co/Pd bilayers, with the weaker SOC, but only at temperatures of $T = 100$ K and lower. Although this explanation is plausible, the origin of such a discrepancy and the conditions for the validity of the PT approach in the MCA calculations need further investigation.

To test how the finite temperature improves the convergence of the MCA energy, the integration over the BZ is done using various numbers $N_{2D} = (2N_k + 1) \times (2N_k + 1)$ of **k** points which form a square grid with N_k divisions along the $\overline{\Gamma}$–$\overline{X}$ line (at $T = 0$ each grid cell is divided into two triangles to apply the triangle method). The improvement is clearly seen in the FT results for a Co/Pd bilayer in Fig. 11(a) where the variation of E_{MCA} versus N_k is largest for $T = 0$ and becomes smaller with increasing the temperature. At $T = 300$ K, the accuracy of 0.01 meV/(surface atom) is reached with $N_k =$ 30–40 while a much finer **k**-point grid with $N_k = 70$–100 is needed to obtain this accuracy level at $T = 50$ K and $T = 0$. A similar convergence trend is found for the MCA energies calculated for the Co/Pd bilayer with the PT [Figs. 11(b) and 11(c)]; however, for some Co thicknesess, the MCA energy does not fully converge even with $N_k = 100$ ($N_{2D} \approx 40\,000$) at $T = 50$ K and $T = 0$. In particular, although the variation of E_{MCA} at $T = 0$ is a quite moderate in the whole considered interval of $20 \leqslant N_k \leqslant 100$ and even much weaker than for $T = 50$–150 K in the range $20 \leqslant N_k \leqslant 50$, it does not necessarily settle down within the 0.01 meV/(surface atom) margin for larger N_k up to 100.

IV. CONCLUSIONS

The presented theoretical analysis of how the band energy of a layered system is perturbed by the SOC at zero temperature gives a very good insight into the origin of intraband contributions to this energy and, consequently, to the MCA energy defined as the difference of the band energies for two different magnetization directions. The net second-order intraband term of the band energy, which accompanies its usual interband term of the same order, is finite only for systems without the inversion symmetry and determined by the electron states at the FS. More specifically, this term is given, at $T = 0$, by the sum of line integrals over all FS sheets which are curves in the two-dimensional BZ. It is revealed that such a form of the intraband term results from the changes of the FS due to the SOC. This perturbation leads to small shifts of the FS sheet curves which result in additional contributions to the system band energy from the narrow stripelike regions

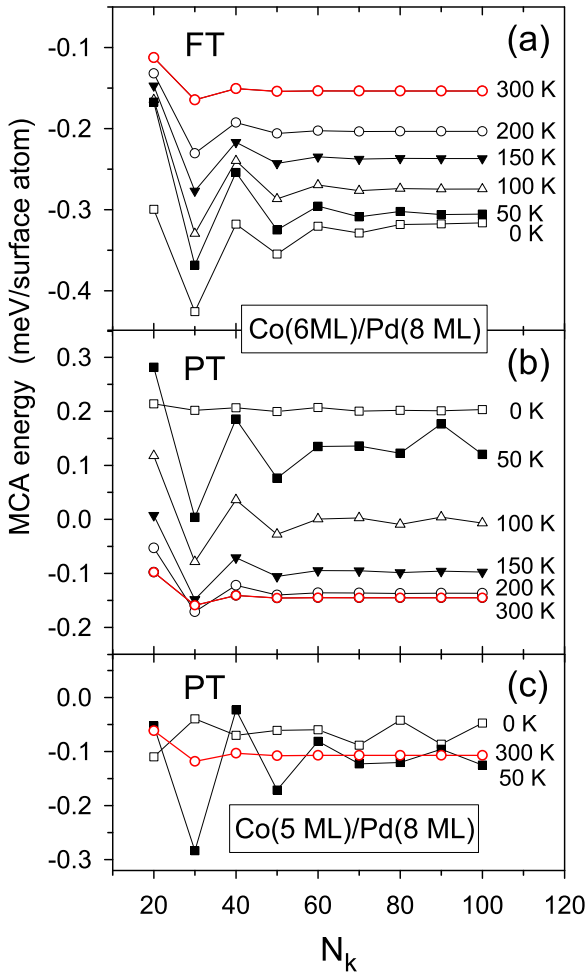

FIG. 11. MCA energy obtained for the (001) (a), (b) fcc Co(6 ML)/Pd(8 ML) and (c) Co(5 ML)/Pd(8 ML) bilayers with the (a) FT and (b), (c) PT at various temperatures versus the number $N_{2D} = (2N_k + 1) \times (2N_k + 1)$ of **k** points used for the integration over the BZ.

of the BZ between the perturbed and unperturbed FS sheets. In the leading order, both the width of each stripe at a specific **k** point of the respective FS sheet and the deviation of the energy of the corresponding band $n\sigma$ from the Fermi level near this point within the stripe are proportional to the first-order correction $\epsilon_{n\sigma}^{(1)}$ to the electron energy $\epsilon_{n\sigma}$ at the **k** point and vary along the stripe. As a result, the net contribution from the stripe to the system energy is proportional to the line integral of the square of $\epsilon_{n\sigma}^{(1)}$, multiplied by the inverse of the band slope which also affects the FS stripe width. These findings, visualized with the relevant schematic illustrations shown in Figs. 1 and 2, clearly explain the mechanism of how the second-order intraband terms arise in the system band energy and, thus, also the MCA energy.

The reported results of the numerical tests prove that the inclusion of the intraband terms in the PT expression for the MCA energy, which are finite for systems without the inversion symmetry, is vital for Co/X bilayers with both moderate (X = Cu) and strong (X = Pd) SOC in the nonmagnetic layer. Indeed, the intraband term of the MCA energy has the magnitude comparable to its interband term and, in fact, both terms have much larger magnitude than the MCA energy itself since they largely cancel out each other. This is true even if the strength of the SOC is artificially reduced to zero in the nonmagnetic layers of X = Cu and Pd. Thus, the presence of the MCA intraband term is primarily due to the lack of the inversion symmetry in the atomic structure of a specific system, and is not the result of an asymmetrical spatial distribution of the SOC inside the system. Nevertheless, the magnitude of this term can be strongly affected, in a similar way as the interband term, by the SOC of a nonmagnetic layer with the d states at the Fermi level, as this is the case for the Co/Pd bilayer.

Further, it is confirmed that the known representation of the MCA energy as half the difference of the SOC energies for two magnetization directions is also valid for systems without the inversion symmetry since its PT expansion reproduces, in the leading order, the extended PT formula for the MCA energy with finite intraband terms included. This alternative approximate, yet very accurate, representation of the MCA energy, was previously [41] derived by assuming that the ground state of the perturbed system is the perturbed ground state of the unperturbed system so that all occupied electron states remain occupied after the SOC perturbation (a one-electron interaction) is applied. This assumption was also made in the original derivation of the PT expression for the MCA energy in Ref. [28] and leads to the formula including only the interband contributions coming from the second-order corrections to the electron energies. However, such an assumption about the ground state is not generally true for extended systems (like the considered bilayers) with continuous energy spectrum since the occupations of some of electron states close to the Fermi level can change upon introducing the SOC perturbation so that the ground state of the perturbed system is then, in fact, one of perturbed excited states of the unperturbed system. Here, we refer to many-electron states (ground and excited) of noninteracting (Kohn-Sham) systems considered in the DFT and these states are the Slater determinants formed of occupied one-electron states.

The questioned assumption was also used, though in a different form, in the state-tracking technique [61] where the choice of the set of occupied electron states in the presence of the SOC is done by maximizing the total projection of the states from this set onto the set of occupied unperturbed states. This technique was proposed to ensure convergence of the MCA energies computed with the FT at $T = 0$; however, its efficiency has been demonstrated only for systems with the inversion symmetry, like Co and Fe films as well as Pd/Co/Pd and Cu/Co/Cu symmetric trilayers [61–63]) where the MCA energy intraband term, neglected due to the mentioned assumption, vanishes anyway. Thus, the validity of the state-tracking approach needs to be reconsidered for systems without the inversion symmetry where such a term is finite and comes from the electron states whose occupancy has changed upon the introduction of the SOC perturbation.

Another key quantity which, apart from the MCA energy, describes magnetic systems and includes both interband and intraband contributions due to the SOC is the Gilbert damping constant determined within the Kamberský model [64,65]. However, significant differences between the two quantities

exist. The contributions to the damping constant are given by the squared moduli of the matrix elements of the spin-orbit torque operator between the perturbed electron states $|m\mathbf{k}\rangle$ so that the intraband contributions, corresponding to the diagonal elements, do not vanish even for systems with the inversion symmetry, like bulk crystals and thin films of ferromagnetic metals of Fe, Co, and Ni [65,66]. This is not the case for the MCA energy whose intraband contributions vanish in the presence of the inversion symmetry because they are determined with the diagonal matrix elements of the SOC operator between the *unperturbed* electron states $|n\mathbf{k}\sigma\rangle$.

Let us also note that, although the system band energy (or the free energy) includes a finite second-order intraband term for layered systems without the inversion symmetry, the first-order term of this energy vanishes even in the absence of such a symmetry provided that the system magnetization has a collinear (ferromagnetic) configuration since, in this case, the first-order corrections to the energies of electrons with opposite wave vectors ($\mathbf{k}$ and $-\mathbf{k}$) cancel out. However, such a cancellation does not take place in systems with a noncollinear magnetization (like chiral magnetic structures) where the first-order terms of their band energies are finite and this gives rise to the Dzyaloshinskii-Moriya interaction [52].

APPENDIX A: CORRECTION TO FERMI ENERGY DUE TO SPIN-ORBIT COUPLING IN PERTURBATION THEORY

The change $\delta\epsilon_{\rm F} = \epsilon_{\rm F} - \epsilon_{\rm F0}$ of the Fermi energy due to the SOC can be determined from the condition that the number of electrons N remains unchanged upon the introduction of the perturbation. It can be achieved by expanding the occupation factor $f(\epsilon_m) = f(\epsilon_{n\sigma} + \delta\epsilon_{n\sigma}) = f_0(\epsilon_{n\sigma} + \delta\epsilon_{n\sigma} - \delta\epsilon_{\rm F})$ in the power series of $\delta\epsilon_{n\sigma} - \delta\epsilon_{\rm F}$ in the expression that defines N in Eq. (4) and, subsequently, determining $\delta\epsilon_{\rm F}$ from the resulting equation. This leads to the formula [6]

$$\delta\epsilon_{\rm F} = \left[\int d\mathbf{k} \sum_{n\sigma} f_0'(\epsilon_{n\sigma})\epsilon_{n\sigma}^{(2)} + \frac{1}{2}\int d\mathbf{k} \sum_{n\sigma} f_0''(\epsilon_{n\sigma})\big[\epsilon_{n\sigma}^{(1)}\big]^2\right] \Bigg/ \int d\mathbf{k} \sum_{n\sigma} f_0'(\epsilon_{n\sigma}), \tag{A1}$$

once terms of the third and higher orders in the SOC are neglected. Thus, we conclude that the change of the Fermi energy $\delta\epsilon_{\rm F}$ (its leading term) is of the second order in the SOC, both in the presence of the inversion symmetry (leading to $\epsilon_{n\sigma}^{(1)} = 0$), and its absence (with finite $\epsilon_{n\sigma}^{(1)}$ possible).

This conclusion also holds at $T = 0$ which provides justification for neglecting the term $(\delta\epsilon_{\rm F})^2$ in Eqs. (29) and (32). Indeed, in the $T \to 0$ limit, Eq. (A1) takes the form

$$\lim_{T\to 0} \delta\epsilon_{\rm F} = \left[\int d\mathbf{k} \sum_{n\sigma} \delta(\epsilon_{n\sigma} - \epsilon_{\rm F0})\epsilon_{n\sigma}^{(2)} + \frac{1}{2}\int d\mathbf{k} \sum_{n\sigma} \delta'(\epsilon_{n\sigma} - \epsilon_{\rm F0})\big[\epsilon_{n\sigma}^{(1)}\big]^2\right] \Bigg/ \int d\mathbf{k} \sum_{n\sigma} \delta(\epsilon_{n\sigma} - \epsilon_{\rm F0}), \tag{A2}$$

where the integration over the BZ can be reduced to the set of the FS sheets $\mathcal{C}_{n\sigma}$ due to the presence of the Dirac delta function. For each point $\mathbf{k}_s \in \mathcal{C}_{n\sigma}$, this function can be represented as

$$\delta(\epsilon_{n\sigma}(\mathbf{k}) - \epsilon_{\rm F0}) = \frac{\delta(q_\perp)}{|\nabla_{\mathbf{k}}\epsilon_{n\sigma}(\mathbf{k}_s)|} \tag{A3}$$

for the points $\mathbf{k} = \mathbf{k}_s + q_\perp \mathbf{e}_\perp$ along the $q_\perp$ axis parallel to the gradient $\nabla_{\mathbf{k}}\epsilon_{n\sigma} = |\nabla_{\mathbf{k}}\epsilon_{n\sigma}|\mathbf{e}_\perp$ at $\mathbf{k}_s$ and thus perpendicular to the tangent of the curve $\mathcal{C}_{n\sigma}$; see Eq. (18). This provides immediate results for the integrals over $q_\perp$ in the terms involving the function $\delta(\epsilon_{n\sigma}(\mathbf{k}) - \epsilon_{\rm F0})$ (but not its derivative) in Eq. (A2). Furthermore, by differentiating Eq. (A3) with respect to $q_\perp$ we find

$$\delta'(\epsilon_{n\sigma}(\mathbf{k}) - \epsilon_{\rm F0}) = \frac{\delta'(q_\perp)}{|\nabla_{\mathbf{k}}\epsilon_{n\sigma}(\mathbf{k}_s)|\partial\epsilon_{n\sigma}/\partial q_\perp(\mathbf{k}_s)} = \frac{\delta'(q_\perp)}{|\nabla_{\mathbf{k}}\epsilon_{n\sigma}(\mathbf{k}_s)|^2} \tag{A4}$$

since, for the assumed orientation of the $q_\perp$ axis, the derivative $\partial\epsilon_{n\sigma}/\partial q_\perp(\mathbf{k}_s)$ is positive and equal to $|\nabla_{\mathbf{k}}\epsilon_{n\sigma}(\mathbf{k}_s)|$. The integral over $q_\perp$ of the above expression multiplied by $[\epsilon_{n\sigma}^{(1)}]^2$ can then be done by integration by parts and includes factor $\partial\epsilon_{n\sigma}^{(1)}/\partial q_\perp$ which can also be represented as $\nabla_{\mathbf{k}}\epsilon_{n\sigma}^{(1)} \cdot \mathbf{e}_\perp$. As a result, we arrive at the following expression for the shift of the Fermi energy due to the SOC at zero temperature:

$$\lim_{T\to 0} \delta\epsilon_{\rm F} = \sum_{n\sigma} \int_{\mathcal{C}_{n\sigma}} ds \left[\frac{\epsilon_{n\sigma}^{(2)}}{|\nabla_{\mathbf{k}}\epsilon_{n\sigma}(\mathbf{k}_s)|} - \frac{\epsilon_{n\sigma}^{(1)}[\nabla_{\mathbf{k}}\epsilon_{n\sigma}^{(1)} \cdot \mathbf{e}_\perp]}{|\nabla_{\mathbf{k}}\epsilon_{n\sigma}(\mathbf{k}_s)|^2}\right] \Bigg/ \sum_{n\sigma} \int_{\mathcal{C}_{n\sigma}} ds \frac{1}{|\nabla_{\mathbf{k}}\epsilon_{n\sigma}(\mathbf{k}_s)|}, \tag{A5}$$

where all terms are finite and the shift itself is of the second order in the SOC. Note that the denominator (after dividing it by $\Omega_{\rm 2D}$) in Eqs. (A2) and (A5) is equal to the DOS $n(\epsilon_{\rm F0})$ at the Fermi level in the unperturbed system.

However, as it was noted in the case of the MCA energy, a formula like above, including the sum over many sheets of the FS is computationally very cumbersome and the finite-temperature expression (A1) should be used instead if one wants to calculate the shift of the Fermi energy within the PT approach. Alternatively, one could perform the calculations of $\delta\epsilon_{\rm F}$ at $T = 0$ by applying the triangular method [1,56] to calculate the integrals over the two-dimensional wave $\mathbf{k}$ for each energy band $n\sigma$ in Eq. (A2). However, this method is still more complex than the finite-temperature approach using Eq. (A1) which is the most convenient way for such a calculation with the PT.

APPENDIX B: ALTERNATIVE DERIVATION OF SECOND-ORDER INTRABAND TERM OF MCA ENERGY AT $T = 0$

The occupied band energies of the unperturbed and perturbed systems at $T = 0$ can be expressed with the electron energies $\epsilon_{n\sigma}$, $\epsilon^{\rm per}_{n\sigma}$ and the corresponding Fermi energies $\epsilon_{\rm F0}$, $\epsilon_{\rm F}$ using the unit step function θ:

$$E^{(0)}_{\rm b} = \frac{1}{\Omega_{\rm 2D}} \int d\mathbf{k} \sum_{n\sigma} \theta(\epsilon_{\rm F0} - \epsilon_{n\sigma})\epsilon_{n\sigma}, \tag{B1}$$

$$E_{\rm b} = \frac{1}{\Omega_{\rm 2D}} \int d\mathbf{k} \sum_{n\sigma} \theta\big(\epsilon_{\rm F} - \epsilon^{\rm per}_{n\sigma}\big)\epsilon^{\rm per}_{n\sigma}. \tag{B2}$$

The change of the band energy due to the SOC perturbation at $T = 0$ can then be represented as follows:

$$\Omega_{\rm 2D}\big(E_{\rm b} - E^{(0)}_{\rm b}\big) = \int d\mathbf{k} \sum_{n\sigma} \theta\big(\epsilon_{\rm F} - \epsilon^{\rm per}_{n\sigma}\big)\big(\epsilon^{\rm per}_{n\sigma} - \epsilon_{\rm F0}\big) - \int d\mathbf{k} \sum_{n\sigma} \theta(\epsilon_{\rm F0} - \epsilon_{n\sigma})(\epsilon_{n\sigma} - \epsilon_{\rm F0}) \tag{B3}$$

after subtracting the term

$$\int d\mathbf{k} \sum_{n\sigma} \theta\big(\epsilon_{\rm F} - \epsilon^{\rm per}_{n\sigma}\big) - \int d\mathbf{k} \sum_{n\sigma} \theta(\epsilon_{\rm F0} - \epsilon_{n\sigma}) = 0 \tag{B4}$$

multiplied by $\epsilon_{\rm F0}$. This term vanishes because it is equal (after dividing it by $\Omega_{\rm 2D}$) to the difference of the numbers of occupied electron states in the perturbed and unperturbed systems while these numbers are identical since they are equal to the fixed number of electrons N in the system.

Further, the occupation factor, with $\epsilon^{\rm per}_{n\sigma} = \epsilon_{n\sigma} + \delta\epsilon_{n\sigma}$ and $\epsilon_{\rm F} = \epsilon_{\rm F0} + \delta\epsilon_{\rm F}$, can be expanded in a power series with linear and quadratic terms included:

$$\theta\big(\epsilon_{\rm F} - \epsilon^{\rm per}_{n\sigma}\big) = \theta(\epsilon_{\rm F0} - \epsilon_{n\sigma}) + \delta(\epsilon_{\rm F0} - \epsilon_{n\sigma})(\delta\epsilon_{\rm F} - \delta\epsilon_{n\sigma}) + \tfrac{1}{2}\delta'(\epsilon_{\rm F0} - \epsilon_{n\sigma})(\delta\epsilon_{\rm F} - \delta\epsilon_{n\sigma})^2 \tag{B5}$$

which, multiplied by $\epsilon^{\rm per}_{n\sigma} - \epsilon_{\rm F0} = \epsilon_{n\sigma} - \epsilon_{\rm F0} + \delta\epsilon_{n\sigma}$ in Eq. (B3), leads to

$$\begin{aligned}\Omega_{\rm 2D}\big(E_{\rm b} - E^{(0)}_{\rm b}\big) = {} & \int d\mathbf{k} \sum_{n\sigma} \theta(\epsilon_{\rm F0} - \epsilon_{n\sigma})\delta\epsilon_{n\sigma} + \int d\mathbf{k} \sum_{n\sigma} \delta(\epsilon_{\rm F0} - \epsilon_{n\sigma})(\epsilon_{n\sigma} - \epsilon_{\rm F0})(\delta\epsilon_{\rm F} - \delta\epsilon_{n\sigma}) \\ & + \delta\epsilon_{\rm F} \int d\mathbf{k} \sum_{n\sigma} \delta(\epsilon_{\rm F0} - \epsilon_{n\sigma})\delta\epsilon_{n\sigma} - \int d\mathbf{k} \sum_{n\sigma} \delta(\epsilon_{\rm F0} - \epsilon_{n\sigma})(\delta\epsilon_{n\sigma})^2 \\ & + \frac{1}{2} \int d\mathbf{k} \sum_{n\sigma} \delta'(\epsilon_{\rm F0} - \epsilon_{n\sigma})(\epsilon_{n\sigma} - \epsilon_{\rm F0})(\delta\epsilon_{\rm F} - \delta\epsilon_{n\sigma})^2 + \frac{1}{2} \int d\mathbf{k} \sum_{n\sigma} \delta'(\epsilon_{\rm F0} - \epsilon_{n\sigma})\delta\epsilon_{n\sigma}(\delta\epsilon_{\rm F} - \delta\epsilon_{n\sigma})^2. \end{aligned} \tag{B6}$$

The second term on the right-hand side vanishes since the Dirac delta function satisfies the relation $x\delta(x) = 0$ (here for $x = \epsilon_{\rm F0} - \epsilon_{n\sigma}$), the third term with $\delta\epsilon_{n\sigma}$ represented with $\epsilon^{(1)}_{n\sigma}$ only also vanishes due to the cancellation of $\mathbf{k}$ and $-\mathbf{k}$ contributions. The remaining part of the third term (including $\epsilon^{(2)}_{n\sigma}$) and the last term can be both neglected as they are of the third or higher orders in the SOC. As a result, the above expression is reduced to the sum

$$\begin{aligned}\Omega_{\rm 2D}\big(E_{\rm b} - E^{(0)}_{\rm b}\big) = {} & \int d\mathbf{k} \sum_{n\sigma} \theta(\epsilon_{\rm F0} - \epsilon_{n\sigma})\delta\epsilon_{n\sigma} - \int d\mathbf{k} \sum_{n\sigma} \delta(\epsilon_{\rm F0} - \epsilon_{n\sigma})(\delta\epsilon_{n\sigma})^2 \\ & + \frac{1}{2} \int d\mathbf{k} \sum_{n\sigma} \delta'(\epsilon_{\rm F0} - \epsilon_{n\sigma})(\epsilon_{n\sigma} - \epsilon_{\rm F0})(\delta\epsilon_{\rm F} - \delta\epsilon_{n\sigma})^2 \end{aligned} \tag{B7}$$

which can be further simplified by dividing its last term into the following three parts:

$$\begin{aligned} & \frac{1}{2}(\delta\epsilon_{\rm F})^2 \int d\mathbf{k} \sum_{n\sigma} \delta'(\epsilon_{\rm F0} - \epsilon_{n\sigma})(\epsilon_{n\sigma} - \epsilon_{\rm F0}) \\ & - \delta\epsilon_{\rm F} \int d\mathbf{k} \sum_{n\sigma} \delta'(\epsilon_{\rm F0} - \epsilon_{n\sigma})(\epsilon_{n\sigma} - \epsilon_{\rm F0})\delta\epsilon_{n\sigma} \\ & + \frac{1}{2} \int d\mathbf{k} \sum_{n\sigma} \delta'(\epsilon_{\rm F0} - \epsilon_{n\sigma})(\epsilon_{n\sigma} - \epsilon_{\rm F0})(\delta\epsilon_{n\sigma})^2 \end{aligned} \tag{B8}$$

and noting that the first part, including $(\delta\epsilon_{\rm F})^2 = O(H^4_{\rm SO})$, can be neglected while the second part, with $\delta\epsilon_{n\sigma} \approx \epsilon^{(1)}_{n\sigma}$ again vanishes due to the cancellation of the $\mathbf{k}$ and - $\mathbf{k}$ contributions. Thus, the following expression is obtained:

$$\begin{aligned}\Omega_{\rm 2D}(E_{\rm b} - E^{(0)}_{\rm b}) = {} & \int d\mathbf{k} \sum_{n\sigma} \theta(\epsilon_{\rm F0} - \epsilon_{n\sigma})\delta\epsilon_{n\sigma} \\ & - \int d\mathbf{k} \sum_{n\sigma} \delta(\epsilon_{\rm F0} - \epsilon_{n\sigma})(\delta\epsilon_{n\sigma})^2 \\ & - \frac{1}{2} \int d\mathbf{k} \sum_{n\sigma} \delta'(\epsilon_{\rm F0} - \epsilon_{n\sigma})(\epsilon_{\rm F0} - \epsilon_{n\sigma}) \\ & \times (\delta\epsilon_{n\sigma})^2. \end{aligned} \tag{B9}$$

Now, we can again make use of the general relation $x\delta(x) = 0$ which after differentiating with respect to x gives the formula $x\delta'(x) = -\delta(x)$ which allows for rephrasing the last term. In

this way, we arrive at the following expression:

$$E_{\rm b} - E_{\rm b}^{(0)} = \frac{1}{\Omega_{\rm 2D}} \int d\mathbf{k} \sum_{n\sigma} \theta(\epsilon_{\rm F0} - \epsilon_{n\sigma}) \delta\epsilon_{n\sigma} - \frac{1}{2} \frac{1}{\Omega_{\rm 2D}} \int d\mathbf{k} \sum_{n\sigma} \delta(\epsilon_{\rm F0} - \epsilon_{n\sigma}) (\delta\epsilon_{n\sigma})^2 \quad \text{(B10)}$$

which after the substitution $\delta\epsilon_{n\sigma} = \epsilon_{n\sigma}^{(1)} + \epsilon_{n\sigma}^{(2)}$ and neglecting terms of the third and higher orders takes the form

$$\begin{aligned} E_{\rm b} - E_{\rm b}^{(0)} &= \frac{1}{\Omega_{\rm 2D}} \int d\mathbf{k} \sum_{n\sigma} \theta(\epsilon_{\rm F0} - \epsilon_{n\sigma}) \epsilon_{n\sigma}^{(1)} \\ &\quad + \frac{1}{\Omega_{\rm 2D}} \int d\mathbf{k} \sum_{n\sigma} \theta(\epsilon_{\rm F0} - \epsilon_{n\sigma}) \epsilon_{n\sigma}^{(2)} \\ &\quad - \frac{1}{2} \frac{1}{\Omega_{\rm 2D}} \int d\mathbf{k} \sum_{n\sigma} \delta(\epsilon_{n\sigma} - \epsilon_{\rm F0}) \big(\epsilon_{n\sigma}^{(1)}\big)^2 \\ &= E_{\rm b}^{(1)} + E_{\rm b}^{(2)} + E_{\rm b}^{(2')}, \end{aligned} \quad \text{(B11)}$$

where the relation $\delta(x) = \delta(-x)$ with $x = \epsilon_{\rm F0} - \epsilon_{n\sigma}$ has been also applied. Since the first-order term vanishes, $E_{\rm b}^{(1)} = 0$, this finally shows that the change of the band energy of layered systems is the sum of the second-order interband and intraband terms:

$$E_{\rm b} - E_{\rm b}^{(0)} = E_{\rm b}^{(2)} + E_{\rm b}^{(2')}. \quad \text{(B12)}$$

The intraband term $E_{\rm b}^{(2')}$ has exactly the same form as in Eq. (17) derived in Sec. II B by taking the $T \to 0$ limit of $F_{\rm intra}^{(2)}$ and can be further represented by the sum of the line integrals over all FS sheets as in Eq. (33) obtained by the calculation of $E_{\rm b}$ at $T = 0$ based on Eq. (22). Although the derivation presented in this Appendix is mathematically rigorous, the physical origin of the extra second-order term $E_{\rm b}^{(2')}$, due to intraband contributions, is much better elucidated by the way this term is derived and interpreted in the main text.

[1] M. Cinal, D. M. Edwards, and J. Mathon, Phys. Rev. B **50**, 3754 (1994).
[2] L. Szunyogh, B. Újfalussy, C. Blaas, U. Pustogowa, C. Sommers, and P. Weinberger, Phys. Rev. B **56**, 14036 (1997).
[3] M. Cinal, J. Phys.: Condens. Matter **15**, 29 (2003).
[4] L. M. Sandratskii, Phys. Rev. B **92**, 134414 (2015).
[5] S. Manna, P. L. Gastelois, M. Dabrowski, P. Kuświk, M. Cinal, M. Przybylski, and J. Kirschner, Phys. Rev. B **87**, 134401 (2013).
[6] M. Cinal, Phys. Rev. B **105**, 104403 (2022).
[7] M. Cinal and D. M. Edwards, Phys. Rev. B **57**, 100 (1998).
[8] M. Cinal, J. Phys.: Condens. Matter **13**, 901 (2001).
[9] M. Cinal and D. M. Edwards, Phys. Rev. B **55**, 3636 (1997).
[10] C. H. Chang, K. P. Dou, G. Y. Guo, and C. C. Kaun, NPG Asia Mater. **9**, e424 (2017).
[11] D. M. Edwards, J. Mathon, R. B. Muniz, and M. S. Phan, Phys. Rev. Lett. **67**, 493 (1991); **67**, 1476(E) (1991).
[12] J. Li, M. Przybylski, F. Yildiz, X. D. Ma, and Y. Z. Wu, Phys. Rev. Lett. **102**, 207206 (2009).
[13] U. Bauer, M. Dabrowski, M. Przybylski, and J. Kirschner, Phys. Rev. B **84**, 144433 (2011).
[14] M. Przybylski, M. Dabrowski, U. Bauer, M. Cinal, and J. Kirschner, J. Appl. Phys. **111**, 07C102 (2012).
[15] S. Manna, M. Przybylski, D. Sander, and J. Kirschner, J. Phys.: Condens. Matter **28**, 456001 (2016).
[16] M. Jamali, K. Narayanapillai, X. Qiu, L. M. Loong, A. Manchon, and H. Yang, Phys. Rev. Lett. **111**, 246602 (2013).
[17] J. Yu, X. Qiu, Y. Wu, J. Yoon, P. Deorani, J. M. Besbas, A. Manchon, and H. Yang, Sci. Rep. **6**, 32629 (2016).
[18] M. Belmeguenai, Y. Roussigné, S. M. Chérif, A. Stashkevich, T. Petrisor Jr, M. Nasui, and M. S. Gabor, J. Phys. D: Appl. Phys. **52**, 125002 (2019).
[19] A. K. Dhiman, M. Matczak, R. Gieniusz, I. Sveklo, Z. Kurant, U. Guzowska, F. Stobiecki, and A. Maziewski, J. Magn. Magn. Mater. **519**, 167485 (2021).
[20] R. Gieniusz, P. Mazalski, U. Guzowska, I. Sveklo, J. Fassbender, A. Wawro, and A. Maziewski, J. Magn. Magn. Mater. **537**, 168160 (2021).
[21] W. S. Ham, A. M. Pradipto, K. Yakushiji, K. Kim, S. H. Rhim, K. Nakamura, Y. Shiota, S. Kim, and T. Ono, npj Comput. Mater. **7**, 129 (2021).
[22] Y. Wei, C. Liu, Z. Zeng, X. Wang, J. Wang, and Q. Liu, J. Magn. Magn. Mater. **521**, 167507 (2021).
[23] M. Weinert, R. E. Watson, and J. W. Davenport, Phys. Rev. B **32**, 2115 (1985).
[24] X. Wang, D. S. Wang, R. Wu, and A. J. Freeman, J. Magn. Magn. Mater. **159**, 337 (1996).
[25] B. Dieny and M. Chshiev, Rev. Mod. Phys. **89**, 025008 (2017).
[26] P. V. Ong, N. Kioussis, P. K. Amiri, and K. L. Wang, Phys. Rev. B **94**, 174404 (2016).
[27] K. Masuda and Y. Miura, Phys. Rev. B **98**, 224421 (2018).
[28] P. Bruno, Phys. Rev. B **39**, 865 (1989).
[29] D. S. Wang, R. Wu, and A. J. Freeman, Phys. Rev. B **47**, 14932 (1993).
[30] G. Autès, C. Barreteau, D. Spanjaard, and M.-C. Desjonquères, J. Phys.: Condens. Matter **18**, 6785 (2006).
[31] D. Li, C. Barreteau, and A. Smogunov, Phys. Rev. B **93**, 144405 (2016).
[32] Y. Miura, S. Ozaki, Y. Kuwahara, M. Tsujikawa, K. Abe, and M. Shirai, J. Phys.: Condens. Matter **25**, 106005 (2013).
[33] Y. Miura, M. Tsujikawa, and M. Shirai, J. Appl. Phys. **113**, 233908 (2013).
[34] J. Okabayashi, Y. Miura, and H. Munekata, Sci. Rep. **8**, 8303 (2018).
[35] L. Ke, Phys. Rev. B **99**, 054418 (2019).
[36] Y. Miura and J. Okabayashi, J. Phys.: Condens. Matter **34**, 473001 (2022).
[37] D. Li, A. Smogunov, C. Barreteau, F. Ducastelle, and D. Spanjaard, Phys. Rev. B **88**, 214413 (2013).
[38] M. Cinal and A. Umerski, Phys. Rev. B **73**, 184423 (2006).
[39] D. Li, C. Barreteau, M. R. Castell, F. Silly, and A. Smogunov, Phys. Rev. B **90**, 205409 (2014).
[40] C. Barreteau, D. Spanjaard, and M.-C. Desjonquères, C. R. Phys. **17**, 406 (2016).
[41] V. Antropov, L. Ke, and D. Åberg, Solid State Commun. **194**, 35 (2014).

[42] G. Kresse and J. Hafner, Phys. Rev. B **47**, 558 (1993); **49**, 14251 (1994).
[43] G. Kresse and J. Furthmüller, Comput. Mater. Sci. **6**, 15 (1996).
[44] G. Kresse and J. Furthmüller, Phys. Rev. B **54**, 11169 (1996).
[45] M. Blanco-Rey, J. I. Cerdá, and A. Arnau, New J. Phys. **21**, 073054 (2019).
[46] G. Chaudhary, M. S. Dias, A. H. MacDonald, and S. Lounis, Phys. Rev. B **98**, 134404 (2018).
[47] The need to include the intraband terms in the MCA energy for cubic films without mirror symmetry (thus, also lacking the inversion symmetry) was already indicated in Ref. [9]. However, such terms were not further discussed or included in Eq. (19) in that paper which investigated only systems with the inversion symmetry.
[48] E. Abate and M. Asdente, Phys. Rev. **140**, A1303 (1965).
[49] M. Methfessel and A. T. Paxton, Phys. Rev. B **40**, 3616 (1989).
[50] The definition of the grand potential given in Eq. (6) is misprinted in Ref. [6].
[51] Note that the function $g(\epsilon)$ is denoted with the symbol $L(\epsilon)$ in Ref. [9] and the prefactor $-k_{\mathrm{B}}T$ is now included in its definition.
[52] M. Heide, G. Bihlmayer, and S. Blügel, Physica B (Amsterdam) **404**, 2678 (2009).
[53] L. Ke and M. van Schilfgaarde, Phys. Rev. B **92**, 014423 (2015).
[54] M. S. Dresselhaus, G. Dresselhaus, and A. Jorio, *Group Theory. Application to the Physics of Condensed Matter* (Springer, Berlin, 2008).
[55] O. Jepsen, J. Madsen, and O. K. Andersen, Phys. Rev. B **18**, 605 (1978).
[56] C. S. Wang and A. J. Freeman, Phys. Rev. B **19**, 793 (1979).
[57] O. Jepson and O. K. Andersen, Solid State Commun. **9**, 1763 (1971).
[58] J. Rath and A. J. Freeman, Phys. Rev. B **11**, 2109 (1975).
[59] A. R. Mackintosh and O. K. Andersen, in *Electrons at the Fermi Surface*, edited by M. Springford (Cambridge University Press, Cambridge, 1980).
[60] E. Barati, Spin relaxation in magnetic nanostructures, Ph.D. thesis, Institute of Physical Chemistry, Polish Academy of Sciences, 2014, pp. 80–81; https://rcin.org.pl/dlibra/doccontent?id=58139.
[61] D. S. Wang, R. Wu, and A. J. Freeman, Phys. Rev. Lett. **70**, 869 (1993).
[62] D. S. Wang, R. Wu, and A. J. Freeman, Phys. Rev. B **48**, 15886 (1993).
[63] D. S. Wang, R. Wu, and A. J. Freeman, J. Magn. Magn. Mater. **129**, 237 (1994).
[64] V. Kamberský, Czech. J. Phys. B **26**, 1366 (1976).
[65] E. Barati, M. Cinal, D. M. Edwards, and A. Umerski, Phys. Rev. B **90**, 014420 (2014).
[66] K. Gilmore, Y. U. Idzerda, and M. D. Stiles, Phys. Rev. Lett. **99**, 027204 (2007).